



CHAPTER IV

Influence of Surlyn[®] Ionomer Compatibilizer on Phase Morphology, Crystallization Behavior and Thermal Stability of PA6/Surlyn[®]/LDPE Blends

Janya Trimongkol, Manit Nithitanakul*, and John W. Ellis

The Petroleum and Petrochemical College, Chulalongkorn University, Bangkok, Thailand

and

Brian P. Grady

School of Chemical Engineering and Materials Science, University of Oklahoma, Norman, Oklahoma

ABSTRACT

PA6/LDPE blends exhibit phase separation morphology so compatibilization is needed to improve the interfacial adhesion between the phases. In this work, blends of PA6 and LDPE were prepared using a Surlyn[®] ionomer as a compatibilizer. This ionomer type consisted of ethylene segments similar to LDPE structure, and carboxylic groups that are capable of reacting with amide end groups of PA6. This study focused on the effect of Surlyn[®] content on phase morphology, crystallization behavior, and thermal stability of PA6/LDPE blends. The effects were investigated using scanning electron microscopy, thermogravimetric analysis, differential scanning calorimetry, and wide-angle X-ray diffraction. PA6/Surlyn[®] and Surlyn[®]/LDPE were also studied in order to get a better understanding of PA6/LDPE/ionomer blends. The results show that Surlyn[®] is an effective compatibilizer for PA6/LDPE blends as evidenced by a reduction in dispersed phase size and an increase in thermal stability with respect to the values expected from a simple rule of mixing. These results were attributed to: the chemical reactions between PA6 and Surlyn[®]; the effects of Surlyn[®] on LDPE in the amorphous phase, despite the absence of co-crystallization of Surlyn[®] and LDPE; the effect of zinc ions from the Surlyn[®]. It was also found that at a PA6/LDPE blend ratio of 80/20, with 1.5 and 5.0 phr Surlyn[®], the materials had similar degradative properties to that of PA6, thus providing an economically viable way to produce a new material with excellent thermal properties at low cost.

* To whom correspondence should be addressed: E-mail manit.n@chula.ac.th

INTRODUCTION

Polyethylene (PE) and nylon (PA) are two important classes of polymers. PE is relatively inexpensive, easy to process, exhibits good flexibility, and is insensitive to moisture. On the other hand, PA polymers are rigid and possess good barrier properties to oxygen and organic solvents. Although PE is more thermally stable than PA at melt temperatures, PA products can be used at higher temperatures in service [1, 2].

Many attempts have been made to prepare PE/PA blends in an effort to retain the desirable properties of both polymers. However, because of the difference in polarities of the two polymers, unfavorable interactions at the molecular level lead to high interfacial tension and make homogeneous melt mixing of the components difficult. This behavior leads to an unstable morphology and poor interfacial adhesion between phases [3].

The most common way to improve the compatibility of blend components is by introducing a third component, a compatibilizer, in which the chemical structure has similar features to that of both polymers being mixed, or having segments containing reactive centers that can react with both blend constituents [4, 5].

Numerous literature reviews describe the use of ionomer as a class of compatibilizer for PA/PE owing to the strong interaction between ionomer and amide groups of PA (attributed to metal-ion, ion-dipole, chemical bonding, and hydrogen bonding interactions) and the possibility of co-crystallization between the polyethylene segments of the ionomer and the polyethylene segments of the PE [6, 7, 8]. Several types of morphology of PA blends using ionomer as compatibilizer have been studied [6, 7, 8, 9, 10]. The results showed that as little as 0.5 wt% of ionomer produce a maximum reduction of dispersed phase size and also at ionomer contents higher than 5.0 wt% there is no significant reduction in phase size. MacKnight *et al.* [12] found that the reduction in phase size, attributed to a reduction in interfacial tension between the blend phases, was due to amidation reactions between PA and Surlyn[®].

The properties of polymer blends depend on many factors such as blend composition, interfacial tension, particle size, and the characteristics of each blend component. In this work, PA6/LDPE/Surlyn[®] ionomer ternary blends are

investigated in terms of kinetic thermal parameters, co-crystallization behavior, and morphology over a range of compositions. In addition, PA6/Surlyn[®] ionomer and LDPE/Surlyn[®] ionomer are studied in order to get a better understanding of the influence of the compatibilizer in PA6/LDPE/Surlyn[®] ionomer ternary blends

EXPERIMENTAL

Materials

Ultramid B3 polyamide 6 (density 1.31 g/cm³) was obtained from BASF (Thailand) Co., Ltd. Low-density polyethylene, LD 1450 J, an injection molding grade polymer (density 0.914 g/cm³) was kindly supplied by Thai Polyethylene Co., Ltd., and Surlyn[®] 9650 (density 0.95 g/cm³) was supplied by DuPont.

Experimental Procedures

Blending Process

PA6, Surlyn[®], and LDPE were kept in an air-circulating oven at 70 °C for 24 hours to remove moisture. Premixes of PA6/LDPE/ionomer, PA 6/Surlyn[®], and Surlyn[®]/LDPE were prepared at various composition ratios. The concentrations of blends ranged from 20 to 80 wt% and Surlyn[®] contents of 0.5, 1.5, and 5.0 phr were used for the compatibilized blends. These mixtures were melt-blended in a Collin T-20 co-rotating twin-screw extruder using a temperature profile of 75/200/215/220/220/230 °C and a screw rotation speed of 40 rpm. In addition to the blends, pure PA6, Surlyn[®], and LDPE were each passed through the extruder.

Molding Process

Samples for characterization were prepared by compression molding granules of each blend. Granules were preheated at 250 °C by maintaining contact pressure on the material for 3 minutes. Then a force of 10 tons was applied to the mould for a further 3 minutes. Finally, the mould was cooled under pressure to 40 °C before removing the pressed samples. The molded sheets were kept in a vacuum oven for 24 hours at 60 °C before carrying out characterization tests.

Thermogravimetric Analysis

Thermogravimetric and derivative thermogravimetric experiments were carried out using a DuPont 2950 thermogravimetric analyzer. The percent weight

changes were monitored as a function of temperature. Test conditions were: sample weight 10 ± 0.5 mg, temperature range 25 to 600 °C, and three different heating rates (5, 10, 20 °C/min), with heating in air.

Differential Scanning Calorimetric Analysis

A Perkin-Elmer differential scanning calorimeter (DSC-7) was used to analyze the samples. The sample size was 10-13 mg and the following procedure used: (i) first heating run at 80 °C/min, from 30 °C to 250 °C, for deleting the thermal history of the sample; (ii) maintaining the temperature at 250 °C for 5 min; (iii) cooling to room temperature at various cooling rates (5, 10, 20, 40 °C/min); and (iv) second heating run at 10 °C/min, from 30 °C to 250 °C.

Scanning Electron Microscopic Analysis

The samples for SEM analysis were prepared by cryogenically fracturing sheet samples at liquid nitrogen temperature followed by immersion in formic acid to remove the PA6 phase or in decalin to remove the Surlyn[®] phase. Cryogenically fractured surfaces of PA6/LDPE/Surlyn[®], PA6/Surlyn[®], and Surlyn[®]/LDPE were observed by scanning electron microscopy (SEM), using a JEOL (MP 152001) microscope operating at 25kV.

X-ray Diffraction Analysis

Wide-angle X-ray diffraction patterns of all blends were obtained using a Rigaku Rint 2000 diffractometer equipped with a graphite monochromator and a Cu tube for generating CuK α radiation (1.5046 Å). The prepared specimens were mounted on a sample holder (glass slide) and examined between 5° – 40° 2 θ at a scanning rate of 2° 2 θ /min in 0.02° 2 θ increments. Percent crystallinity and amorphous contents were calculated using a deconvoluted gaussian program to separate overlapping peaks.

RESULTS AND DISCUSSION

Morphological analysis

The SEM micrographs of the cryogenically-fractured molded sheets of noncompatibilized PA6/LDPE blends showed the typical morphology of incompatible blends [1, 2, 4, 10, 11, 12] due to the different polarities of molecules.

Fig. 1 micrographs clearly show the two phases of the blends with the dispersed domains being particulate in shape. The lack of interfacial adhesion is evidenced by the large number of craters produced by pulled-out particles formed during the freeze-fractured sample preparation [13]. The domain surfaces and the surfaces of the holes left appear perfectly clean [7,11]. This indicates an absence of adhesion between the matrix and particle surface.

The addition of Surlyn[®] compatibilizer to PA6/LDPE blends resulted in more homogeneous morphologies than noncompatibilized blends (Fig. 2). Fig. 3 shows that the dimensions of the minor phase not only decreased but also attained a more uniform particle size distribution compared with blends without Surlyn[®]. It is evident from Fig. 4 that the presence of Surlyn[®] improved the adhesion between the two phases since there appears to be rough surfaces around the holes and some material has coated the surface of the dispersed particle. Moreover, SEM micrographs indicate that for the case of noncompatibilized PA6/LDPE blends the dispersed phase particles completely fill the holes in the matrix. By contrast, the dispersed domains of compatibilized PA6/LDPE blends fill only the internal part of the holes, leaving a gap between their surface and that of the matrix. This gap between the surfaces in compatibilized blends may be due to some remaining grafted copolymer formed during the melt mixing of PA6 and Surlyn[®]. The grafting of PA6 onto LDPE via the compatibilizer can be verified using the Molau test. This test involves mixing LDPE and PA6 in formic acid to yield dissolved PA6 remaining at the bottom and insoluble PE at the top of the solution. Addition of a polymeric component that is capable of reacting with PA6 end groups and is also miscible with PE leads to the formation of a third phase that appears as a white colloidal suspension in the formic acid [1]. All of the compatibilized PA6/LDPE blend ratios showed white colloidal suspensions in the formic acid.

The diameters of the dispersed particles of the blends were measured by etching the blends in formic acid or decalin to dissolve the minor phase. The number-average phase size of the blends is shown in Table 1. It appeared that particle size increased with increasing concentration of the dispersed phase. The increase in size may be due to phase inversion of the system which itself may be related to the high rate of coalescence at high concentrations and to the high viscosity

of PA6 [13,18]. Moreover, SEM micrographs of etched blends indicate that for PA/LDPE blend compositions of 20/80, 40/60, 50/50, and 60/40, PA6 was found to be the dispersed phase since holes were observed after the blends were immersed in formic acid. The conformity between these results and those of Psarski *et al.* indicates that the phase inversion zone they found in blends of PA6/polyolefin and PA6/acrylic acid grafted polyolefins [4] occurred in PA6/polyolefin at ratios ranging from 50/50 to 70/30. In all the compatibilized PA6/LDPE blends, the dispersed phase particle size decreased with increasing ionomer content. Not only was the extent of dispersed phase particle size reduction more pronounced when PA6 was the dispersed phase but there was also a lower degree of distribution of the minor phase. These effects may be due to the high affinity of Surlyn[®] ionomer for PA6 [12].

The PA6/ Surlyn[®] blend morphology appeared to be homogeneous since no evidence of a dispersed phase could be seen (Fig. 5). By etching the blends a dispersed phase was readily observable (Fig. 6). An increase in Surlyn[®] content in PA6/Surlyn[®] blends caused a decrease in the size of particles, and gave a more homogeneous morphology. The average size of the dispersed phase particles in the PA6/ Surlyn[®] blends was approximately 1 μm , and seemed to vary little with blend composition. The reduction in particle size of the dispersed domains again indicated chemical reactions taking place between phases as confirmed by the Molau test. All PA6/ionomer blends gave white colloidal suspensions with formic acid. In a study of PA and Surlyn[®], Willis *et al.* [13] found that chemical bonding occurred at the interface through amide formation of terminal amine groups of PA and acid functional groups of the ionomer.

Fig. 7 shows micrographs of Surlyn[®]/LDPE blends at various blend ratios. The micrographs do not provide clear evidence of phase-separation at Surlyn[®]/LDPE ratios of 50/50, 60/40, and 80/20. Higher Surlyn[®] contents gave more homogeneous blends. Moreover, Figs. 7 (a) and (b) show the rough surfaces on the holes remaining and some material coating the dispersed particles after cryogenically fracturing, providing evidence of adhesion between the two blend components. These results suggest compatibility of the PE backbone segments of the Surlyn[®] with PE segments of the LDPE. However, it was very difficult to measure the phase particle size because both components dissolve in the same solvents.

It can be concluded from the SEM analysis that the phase particle size of PA6/LDPE blends depended on the blend composition and the Surlyn[®] content. Additionally, it was found that the Surlyn[®] ionomer showed a higher affinity for PA6 than for LDPE resulting in a more homogeneous morphology of PA6/Surlyn[®] blends than Surlyn[®]/LDPE blends.

WAXS analysis

WAXS analysis was performed in order to correlate the crystalline structure of the blends with their chemical composition. The WAXS patterns of PA6/LDPE, PA6/Surlyn[®], and Surlyn[®]/LDPE blends are shown in Figs. 8, 9, and 10, respectively. Pure PA6 gave pronounced 2θ peaks at 20.2° and 23.6° associated with α_1 -form (002) and α_2 -form (200) crystal structures, respectively. A pronounced peak at 21.4° for the γ -form crystal structure was not found. Nevertheless, PA6 produced some slight changes in the intermediate region between (002) and (200) reflections. This intermediate region ($21^\circ < 2\theta < 23^\circ$) corresponds to reflections for the γ -form crystal structure of PA6 [15]. Both pure LDPE and pure ionomer showed pronounced 2θ peaks at 21.5° (110) and 23.8° (200) [4].

The WAXS patterns for noncompatibilized PA6/LDPE, compatibilized PA6/LDPE, PA6/Surlyn[®], and Surlyn[®]/LDPE blends showed peak positions at the same angles as for the pure components. None of the blends produced γ -form crystal structure features, but the intensity of the α_1 -form tended to decrease with increasing second component content for all PA6 blends. The limitation of the peak positions for pure components being the same as for their blends makes it very difficult to use a deconvoluted gaussian program to separate overlapping peaks, which is the method normally used to determine percent crystallinity and amorphous contents of blends. However, Antony *et al.* has shown that the presence of Surlyn[®] increases the amount of amorphous content of such blends [19].

The crystallinity levels of the blends, therefore, were determined from the enthalpies of fusion calculated from DSC experiments.

DSC analysis

Melting and crystallization behaviors of PA6/Surlyn[®] are shown in Fig. 11. PA6 gave a crystallization temperature, T_c , of 180.9 °C and two distinct melting points, T_m , at 210.5 °C and 221.2 °C. PA6 has two distinct crystal structures, a monoclinic α -form crystal structure having a melting temperature of about 221 °C and a γ -form crystalline structure having a melting point around 213 °C [11, 18]. The Surlyn[®] gave a T_m of 94.23 °C. Nevertheless, there was evidence of chemical reactions between PA6 and Surlyn[®] from the Molau test. The data presented in Table 2 indicate that PA6/Surlyn[®] blends were immiscible, since the PA6 and the Surlyn[®] melting endotherms are independent of each other (Fig. 11). Pure Surlyn[®] showed a T_c at 61.3 °C. For PA6/Surlyn[®] blends the T_c peaks of Surlyn[®] shifted to higher temperatures than for pure Surlyn[®], suggesting that PA6 acts as a nucleating agent for Surlyn[®] but that the Surlyn[®] interferes with the ability of PA6 to crystallize. Crystallization peaks corresponding to PA6 could not be observed for PA6/Surlyn[®] blend ratios 20/80, 40/60, 50/50, and 60/40. The Surlyn[®] peaks of fractionated crystallization of PA6/Surlyn[®] for ratios 20/80, 40/60, 50/50, and 60/40 could, however, be observed. These behaviors may be due to chemical reactions between PA6 and Surlyn[®], which could interfere with the ability of PA6 to crystallize. However, the intensity of the γ -form crystal structure peaks decreased with increasing ionomer content since the γ -form crystal structure of PA6 is affected by ionomer content. The percent weight fractional crystallinity, χ_c , was calculated from equation 1,

$$\chi_c = \frac{\Delta H \times 100\%}{\Delta H_f \times wt. \text{ fraction}} \quad (\text{Equation 1})$$

where ΔH is the melting enthalpy of the component present in the blend and ΔH_f is the heat of fusion for 100% crystallinity of the pure component (190 J/g for PA6, and 282 J/g for LDPE).

The wt% fractional crystallinity of PA6/Surlyn[®] blends (Table 2) gave the crystallinity of each component as being approximately the same as for the pure components, since the crystallization of each component was independent of the other in the absence of interactions between components in crystal phase.

In the case of Surlyn[®]/LDPE blends, pure LDPE showed a T_c at 80.4 °C and a T_m at 104.6 °C. The blends gave two melting peaks indicative of Surlyn[®] and LDPE crystal structures. DSC thermograms of Surlyn[®]/LDPE blends are shown in Fig. 12. The Surlyn[®] acted as a nucleating agent for the LDPE as evidenced by a shift in T_c peaks of LDPE to higher temperatures. The shift in Surlyn[®] T_c peaks to lower values than for pure Surlyn[®] was thought to be due to the branching of LDPE interfering with the ability of the Surlyn[®] to crystallize.

The wt % fractional crystallinity of Surlyn[®]/LDPE blends could not be reliably calculated from DSC results due to the large overlapping of the two melting peaks. However, as can be seen from Surlyn[®]/LDPE thermograms (Fig. 12), the intensity of the peaks corresponded to the blend composition since each blend component did not interfere with the crystallization of the other.

Both noncompatibilized and compatibilized PA6/LDPE blends exhibited the characteristic behavior of immiscible blends (Figs. 13 and 14), i.e. they gave two distinct melting peaks. For the noncompatibilized PA6/LDPE blends, crystallization of the LDPE component took place at 90-91 °C, i.e. 10 °C higher than pure LDPE. It appeared that the presence of PA6 acted as nucleating sites and causes crystallization of the LDPE at higher temperatures, thus leading to higher crystallinity than pure LDPE. These results are complied to the finding of Halléd *et al.* [16], who found an increase in the T_c of the PE phase in PA/LDPE blends by 6-8 °C compared with that of pure LDPE.

The addition of a Surlyn[®] compatibilizer to PA6/LDPE blends revealed a slight lowering of the PA6 T_m peaks compared with that of pure PA6. This may be attributed to the nucleating effect of the Surlyn[®], thereby affecting the crystallinity of the PA6. Moreover, the presence of a melting peak at a lower temperature than the melting temperature of pure α -form PA6 indicates the existence of a γ -form crystalline structure in the dispersed phase [4]. For compatibilized blends where LDPE formed the matrix, the LDPE tended to give higher wt% fractional crystallinity. The addition of Surlyn[®] to noncompatibilized blends decreased the size of the dispersed PA6 phase, thus increasing the interface area, thereby promoting crystallization of the LDPE, indicating a nucleating effect promoted by compatibilization [21]. In addition, an increase in the amount of compatibilizer in

the blends caused a decrease in the degree of crystallinity of PA6, especially for the 80/20 blends. This trend may be the result of interactions between PA6 and Surlyn[®], or possibly by hydrogen bonding interfering with the ability of PA6 molecules to crystallize [22].

Even though Surlyn[®] and LDPE have similar structures (Fig. 10) that could possibly co-crystallize, DSC results showed a complete absence of co-crystallization of ionomer/LDPE blends. Grey *et al.* [8] suggests that it is difficult to induce co-crystallization of polymer blends, even in polymers of similar structure. Despite the Surlyn[®]/LDPE morphology indicating compatibility was not found to occur in the crystalline phase; compatibility must therefore exist in either the amorphous phase or at interfaces.

TGA analysis

The analysis of thermal stability and kinetics of degradation of pure components and their blends was based on thermograms obtained from TGA. For the kinetic studies of degradation the fractional conversion was plotted as a function of temperature and then the basic Arrhenius-type expression (Equation 2) used to determine kinetic parameters,

$$da/dt = f(\alpha) A \exp(-E_a/RT) \quad (\text{Equation 2})$$

where A is a pre-exponential factor (represents the rate of degradation at a temperature at which the sample loses a specific weight), E_a is the activation energy (represents the energy barrier for the occurrence of degradation), T is the temperature at a specific weight loss, and R is the gas constant value. Fractional conversion, α , was calculated using Equation 3,

$$\alpha = (w_i - w)/(w_i - w_f) \quad (\text{Equation 3})$$

where w_i is the initial weight of sample, w_f is the final weight of sample, and w is the weight at a particular conversion.

TGA thermograms of pure PA6, Surlyn[®], and LDPE are shown in Fig. 15. The weight of the LDPE sample increased to a maximum and then decreased. The weight increase at the beginning of heating was due to oxygen absorption. The formation of hydroperoxides continued until chain scissions occurred, leading to the formation of volatile low molecular weight compounds [23]. Evolutions of the

volatile materials lead to a weight decrease. However, at the beginning of heating pure PA6 and pure Surlyn[®] an immediate weight decrease was observed. This was due to the loss of absorbed humidity since PA6 and Surlyn[®] are both hygroscopic materials. A fractional conversion of 0.1 was chosen as indicative of the susceptibility of the material to degrade. The temperature at that specific conversion determines the upper temperature limit at which the polymer can be processed. The long induction time observed for LDPE (Fig. 15) showed that it was relatively stable at temperatures below its T_m . However, LDPE is susceptible to oxidation at high processing temperatures [24]. LDPE had lower thermal stability and lower degradation rate than both PA6 and Surlyn[®]. The high degradation rate of Surlyn[®] and PA6 were attributed to the ease of abstraction of carboxylic hydrogen at high temperatures.

Values of degradation temperatures at 0.1 conversion, made independent of heating rate using the Flynn and Wall method [23], are summarized in Tables 4 and 5. These values were determined by plotting degradation temperature at 0.1 conversion as a function of heating rate and then extrapolating to zero heating rate. The Flynn and Wall method is one of the simplest methods of determining rates of degradation using TGA data. The results correlate well with the experimental data on the kinetics of decomposition of blends by the Flynn and Wall method for the initial stage of degradation. This method assumes first order reaction and is based on the kinetic dependence of temperature at which the sample has lost a specific weight.

For noncompatibilized PA6/LDPE blends, the thermal stability of LDPE increased with the addition of PA6, but the blends showed lower thermal characteristics (negative deviations) than predicted from the rule of mixing (Fig. 16). At ratios of 40/60, 50/50 and 60/40, high negative deviation values were observed, attributed to the large particle sizes observed from SEM micrographs. These results are clear evidence of two-phase separation morphology and a lack of interaction between phases in PA6/LDPE blends leading to lower thermal stability than predicted. The degradation temperatures of noncompatibilized PA6/LDPE blends up to a ratio of 20/80 was close to degradation temperature of pure LDPE, and at ratio 80/20 degradation temperatures were close to the degradation temperature of pure PA6. It is known that the initial stage of degradation of immiscible blends is

dominated by the matrix phase [25]. For noncompatibilized PA6/LDPE blends at ratio 50/50 and 60/40, SEM micrographs indicated that the matrix was LDPE, but degradation temperatures were not close to the degradation temperature of pure LDPE. This behavior may be due to the unstable morphology of the blend due to phase inversion where PA6 becomes rich component. The E_a values and increase in degradation rates of the blends correlated with the increase in degradation temperatures.

The degradation temperature of compatibilized blends shifted towards higher temperatures with increasing Surlyn[®] content, and showed positive deviation values from the rule of mixing. This was attributed to the Surlyn[®] improving the interfacial interactions in PA6/LDPE blends. E_a values of compatibilized blends also increased with increasing Surlyn[®] content, which may be attributed to zinc ionic interaction with carboxylic group of PA6. It was thought that this was due to complexation of the zinc ion, which retarded degradation to high temperatures. For 60/40 and 20/80 PA6/LDPE blends compatibilized with Surlyn[®] contents of 1.5 phr and 5.0 phr, the E_a values were close to that of pure PA6. Moreover, synergistic energy barriers were observed for 80/20 PA6/LDPE blends compatibilized with 5.0 phr Surlyn[®]. These results show that at those particular ratios it is possible to obtain a material with thermal degradative properties similar to PA6, thus providing an economically viable way to obtain a material with excellent thermal properties at low cost.

PA6/Surlyn[®] blends showed positive degradation temperature deviations from that predicted by the rule of mixing (Fig. 17), suggesting that chemical reactions between PA6 and Surlyn[®] influenced the thermal behavior. The graph shows that the chemical reactions that occurred at PA6/Surlyn[®] ratios 40/60, 50/50 and 60/40 were higher than those at ratios 20/80 and 80/20. In addition, E_a values of all blend ratios were higher than the E_a of pure PA6, clearly indicating the formation of zinc complex species between the Surlyn[®] and PA6, and also that chemical reactions occurred between them.

Surlyn[®]/LDPE blends (Fig. 18) show, in general, a simple rule of mixing for thermal stability as a function of blend composition. Table 4 shows that the degradation temperatures of Surlyn[®]/LDPE blends are close to that of the Surlyn[®],

indicating that the Surlyn[®] influenced the degradation in the blends. The high positive degradation temperature at a ratio of 80/20 was probably due to Surlyn[®] forming ion complex species, thus shifting degradation to high temperature.

In summary, the thermal stability of PA6/Surlyn[®]/LDPE blends was affected by the chemical structure of the blend components, phase morphology, interactions between phases, and by zinc ion complex species.

CONCLUSIONS

Surlyn[®] compatibilizer, blend composition and the characteristics of the pure components can influence morphology, thermal stability, and crystallization behavior of PA6/LDPE blends.

SEM micrographs of Surlyn[®]/LDPE blends provide some evidence of interactions between phases. Despite the absence of any co-crystallization of Surlyn[®] with LDPE, DSC results indicated that the Surlyn[®] acted as a nucleating agent for LDPE. Although morphology indicating compatibility between Surlyn[®] and LDPE, it was not found to occur in the crystalline phase; compatibility must therefore exist in either the amorphous phase or at interfaces. TGA results of Surlyn[®]/LDPE blends showed thermal stabilities close to those predicted from the rule of mixing.

The SEM micrographs of PA6/Surlyn[®] blends show homogeneous morphology. PA6 acted as a nucleating agent for the blends due to its high crystallization temperature but chemical reactions between PA6 and Surlyn[®] interfered with the ability of PA6 to crystallize. Thermal stabilities of the blends were much higher than that predicted by the rule of mixing. These results indicate that chemical reactions occurred between PA6 and Surlyn[®], and that zinc ion complex species were formed. Surlyn[®] showed a higher affinity for PA6 than for LDPE.

Noncompatibilized PA6/LDPE blends showed a complete absence of any interactions between PA6 and LDPE. However, the thermal stabilities of PA6/LDPE blends were improved by the addition of Surlyn[®]. There is a perturbation of the morphology of PA6 with Surlyn[®] compatibilizer due to the efficiency of the Surlyn[®] to chemically react with PA6 and to undergo interactions with LDPE in the

amorphous phase, but it had little effect on the melting behavior of the blends. TGA results show that for the 80/20 blend ratio of PA6/LDPE with 1.5 and 5.0 phr Surlyn[®], it was possible to obtain a material with similar thermal degradative properties to that of PA6, thus representing an economically viable way to obtain at low cost an alternative to PA6 having excellent thermal properties.

ACKNOWLEDGEMENTS

The author would like to acknowledge TPE Co., Ltd. and BASF Co., Ltd. for kindly providing the LDPE and PA6, respectively, used in this work.

REFERENCES

1. Anttila, U., Hakala, K., Helaja, T., Löfgren, and B., Seppälä, J., *Journal of Polymer Science: Part A; Polymer Chemistry*, 37, 3099-3108 (1999).
2. Kim, B.K., Park, S.Y., and Park S.J. *Eur. Polymer J.*, 27(4/5), 349-354. (1991).
3. Vocke, C., Anttila, U., and Seppälä J., *Journal of Applied Polymer Science*, 72, 1443-1450 (1999).
4. Psaski, M., Pracella, M., and Galeski, A., *Polymer*, 41, 4923-4932.1918-1924 (2000).
5. Jurkowski, B. Kelar, K., and Ciesielska, D., *Journal of Applied Polymer Science*, 69, 713-727 (1998).
6. Cheng, C.C., Fontan, E. Min, K., and White, J.L., *Polymer Engineer and Science*, 28(2), 69-78 (1988).
7. Armet, R. and Moet, A., *Polymer*, 34(5), 977-985 (1993).
8. Fairley, G. and Prud'homme, R.E., *Polymer Engineering and Science*, 27(20), 1495-1503 (1987).
9. Huitric, J., Médéric, P., Moam, M., and Jarrin, J., *Polymer*, 39(20), 4849-4856 (1998).
10. Jurkowski, B., Kelar, K., and Ciesielska, D., *Journal of Applied Polymer Science*, 69, 719-727 (1998).
11. Macknight, W.J., and Lenz, R.W., *Polymer Engineering and Science*, 25(18), 1124-1134 (1985).

12. Willis, J.M. and Favis, B.D., *Polymer Engineering and Science*, 28(21), 1416-1426 (1988).
13. Willis, J.M., Favis, B.D., and Lavallee, C., *Journal of Materials Science*, 28, 1749-1757 (1993).
14. Kelar, K., and Jurkowski, B., *Polymer*, 41, 1055-1062 (2000).
15. Raval, H., Devi, S., Singh, Y.P., and Mehta, M.H., *Polymer*, 32(3), 493-500 (1991).
16. Halléd, A., Ohlsson, B., and Wesslén, B., *Journal of Applied Polymer Science*, 78, 2416-2424 (2000).
17. Sheng, J., Ma, H., Yuan, X.B., Yuan, X.Y., Shen, N.X., and Bian, D.C., *Journal of Applied Polymer Science*, 76, 488-494 (2000).
18. Han, C.D. and Chuang, H. K., *Journal of Applied Polymer Science*, 30, 2431-2455 (1985).
19. Antony, P., Bandyopadhyay, S., and De, S.K., *Polymer*, 41, 787-793 (2000).
20. Samios, C.K., and Kalfoglou, N.K., *Polymer*, 40, 4811-4819 (1999).
21. Silva, E.F., and Soares, B.G., *Journal of Applied Polymer Science*, 60, 1687-1694 (1996).
22. Sánchez, A., Rosales, C., Laredo, E., Müller, A.J., and Pracella M., *Macromol. Chem. Phys.*, 202, 2461-2478 (2001).
23. Mohanty, S., Mukunda, P.G., and Nando, G.B., *Polymer Degradation and Stability*, 50, 21-28 (1995).
24. Bikiaris, D., Prinios, J., Perrier, C., and Panayiotou, C., *Polymer Degradation and Stability*, 57, 313-324 (1997).
25. Lamas, L., Mendez, G.A., Müller, A.J., and Pracella M., *Eur. Polym. J.*, 34(12), 1865-1870 (1998).

LIST OF TABLES

Table 1	Number average diameter of dispersed phase size of blends.
Table 2	Thermal properties of PA6/ Surlyn [®] , and Surlyn [®] /LDPE blends as a function of blend composition
Table 3	Thermal properties of PA6/LDPE blends as a function of blend composition
Table 4	Kinetic parameters of pure components and binary blends
Table 5	Kinetic parameters of PA6/LDPE with 0.5, 1.5, and 5.0 phr Surlyn [®]

Table 1. Number average diameter of dispersed phase size of blends.

Blend type	Number average diameter (μm)					
	Ratio (wt %)	20/80	40/60	50/50	60/40	80/20
Noncompatibilized PA6/LDPE		12.1	20.8	25.7	26.0	22.2
Compatibilized PA6/LDPE with 0.5 phr Surlyn [®]		11.2	12.2	19.1	20.6	2.8
Compatibilized PA6/LDPE with 1.5 phr Surlyn [®]		9.5	10.5	18.1	20.2	2.0
Compatibilized PA6/LDPE with 5.0 phr Surlyn [®]		7.7	8.2	15.7	17.2	1.2
PA6/ Surlyn [®]		0.8	0.5	0.6	0.4	0.2
Surlyn [®] /LDPE*		-	-	-	-	-

* Surlyn[®] and LDPE dissolve in the same solvents.

Table 2. Thermal properties of PA6/ Surlyn[®] and Surlyn[®]/LDPE blends as a function of blend composition.

PA6/ Surlyn [®] (wt %)	Exotherm							Endotherm						
	Onset (°C)	Surlyn [®]			PA6			Surlyn [®]			PA6			
		T _c (°C)	ΔH _c (J/g)	Onset (°C)	T _c (°C)	ΔH _c (J/g)	Onset (°C)	T _m (°C)	χ _c (%)	Onset (°C)	T _m (°C)		χ _c (%)	
											1	2		γ
0/100	66.7	61.3	-	61.6	-	-	-	79.2	94.4	22.4	-	-	-	-
20/80	73.5	68.3	82.6	45.2	-	-	-	79.1	94.7	21.6	208.1	-	220.7	35.2
40/60	74.4	69.3	83.3	18.4	-	-	-	84.5	94.6	22.7	208.6	-	221.0	35.5
50/50	74.4	69.7	85.9	16.5	185.8	181.9	0.6	80.6	93.7	22.3	208.6	-	220.7	34.6
60/40	75.1	69.7	89.7	12.9	185.7	181.4	6.1	82.3	93.4	22.5	211.0	210.3	221.0	35.8
80/20	82.8	70.	-	12.2	186.3	182.6	48.7	87.3	93.7	22.7	211.6	210.8	220.7	35.6
100/0	-	-	-	-	186.3	180.9	64.2	-	-	-	211.7	210.5	221.2	36.4

Surlyn [®] /LDPE (wt %)	Exotherm						Endotherm						
	Onset (°C)	Surlyn [®]			LDPE			LDPE			Surlyn [®]		
		T _c (°C)	ΔH _c (J/g)	onset (°C)	T _c (°C)	ΔH _c (J/g)	Onset (°C)	T _m (°C)	ΔH _m (J/g)	Onset (°C)	T _m (°C)	ΔH _m (J/g)	
													1
0/100	64.9	61.3	65.6	-	-	-	79.7	94.3	41.2	-	-	-	
20/80	69.3	61.9	58.5	97.3	91.7	6.3	82.9	93.8	19.7	100.9	104.8	1.3	
40/60	67.2	60.9	31.7	97.4	91.5	17.7	83.2	93.5	15.0	100.4	104.7	3.5	
50/50	68.2	61.4	39.6	90.5	87.1	26.9	84.6	93.8	11.3	101.1	105.1	12.7	
60/40	65.9	59.5	19.2	96.9	91.3	31.4	-	93.7	-	95.8	104.7	58.1	
80/20	67.8	59.6	9.6	96.7	91.4	41.8	-	93.5	-	95.7	104.6	62.9	
100/0	-	-	-	89.1	84.8	80.4	-	-	-	98.0	104.6	74.3	

Table 3. Thermal properties of PA6/LDPE blends as a function of blend composition.

Blend		Without Surlyn®						With 0.5 phr Surlyn®						With 5.0 phr Surlyn®					
PA6/LDPE		0/100	20/80	40/60	50/50	60/40	80/20	100/0	20/80	40/60	50/50	60/40	80/20	20/80	40/60	50/50	60/40	80/20	
LDPE	Endotherm																		
	Onset (°C)	98.0	98.0	98.5	97.2	96.2	95.6	-	98.5	98.8	98.6	98.8	98.1	98.4	98.8	98.9	98.9	98.2	
	T _m (°C)	104.6	105.2	105.9	104.7	104.6	104.5	-	105.5	104.8	104.3	104.4	104.4	104.6	106.3	104.6	104.4	105.5	
	χ _c (%)	24.3	27.0	25.9	26.8	27.1	12.6	-	28.3	27.9	29.0	31.5	17.6	30.4	31.9	30.1	27.6	31.6	
	Exotherm																		
	Onset (°C)	89.1	96.1	95.7	97.5	97.7	97.7	-	89.1	90.3	90.5	90.9	96.2	88.9	88.4	89.6	91.1	91.9	
	T _c (°C)	80.4	96.1	95.7	97.5	97.7	97.6	-	85.1	85.9	86.5	87.0	90.1	85.1	84.1	86.0	87.9	86.2	
ΔH _c (J/g)	84.7	57.0	46.1	45.6	40.7	11.9	-	60.8	45.0	37.1	35.7	11.0	45.9	32.3	28.8	23.4	10.6		
PA6	Endotherm																		
	Onset (°C)	-	212.5	211.7	211.8	210.3	210.8	211.7	209.9	209.9	211.9	212.6	213.6	209.6	211.3	210.6	212.0	205.2	
	T _m (°C)																		
	γ-form	-	209.9	210.1	210.2	209.8	210.3	210.5	208.3	208.7	210.4	211.2	211.8	-	210.8	208.4	210.9	206.8	
	α-form	-	220.0	220.6	219.9	219.2	219.5	221.2	219.5	219.7	220.7	221.1	221.6	219.4	220.8	219.5	220.8	218.5	
	χ _c (%)	-	25.0	29.2	22.8	20.3	31.6	31.7	36.8	34.8	29.8	27.2	28.3	38.5	36.3	31.1	28.4	29.5	
	Exotherm																		
Onset (°C)	-	185.4	185.2	186.0	184.7	186.7	186.3	183.3	183.8	185.7	185.7	185.6	184.5	180.7	184.3	185.7	182.2		
T _c (°C)	-	181.5	180.8	181.1	179.3	182.7	180.9	178.5	179.6	180.8	182.2	181.9	179.2	176.6	179.7	182.1	176.5		
ΔH _c (J/g)	-	12.4	25.1	26.5	30.7	53.8	64.2	10.9	24.4	28.3	33.7	52.5	6.9	16.2	22.2	31.3	46.6		

Table 4. Kinetic parameters of pure components and binary blends.

Component	Degradation temperature at 0.1 conversion (°C)	E_a (kJ/mol)	$\ln A$ ($\ln \text{min}^{-1}$)
PA6	357.6	127.8	21.9
LDPE	234.8	46.3	6.2
Surlyn [®]	388.7	187.1	30.3
PA6/LDPE blend ratio			
20/80	253.2	47.37	7.3
40/60	259.5	55.84	7.5
50/50	268.4	66.65	8.7
60/40	292.0	50.80	12.6
80/20	328.2	89.32	14.3
PA6/Surlyn [®] blend ratio			
20/80	383	178.1	25.6
40/60	379.4	177.8	27.4
50/50	380.5	171.4	30.0
60/40	379	165.3	36.5
80/20	365.9	157.7	41.7
Surlyn [®] /LDPE blend ratio			
20/80	258	50.2	7.9
40/60	303.9	63.1	9.6
50/50	311.7	71.0	14.8
60/40	327.7	74.2	16.2
80/20	344.8	85.2	19.4

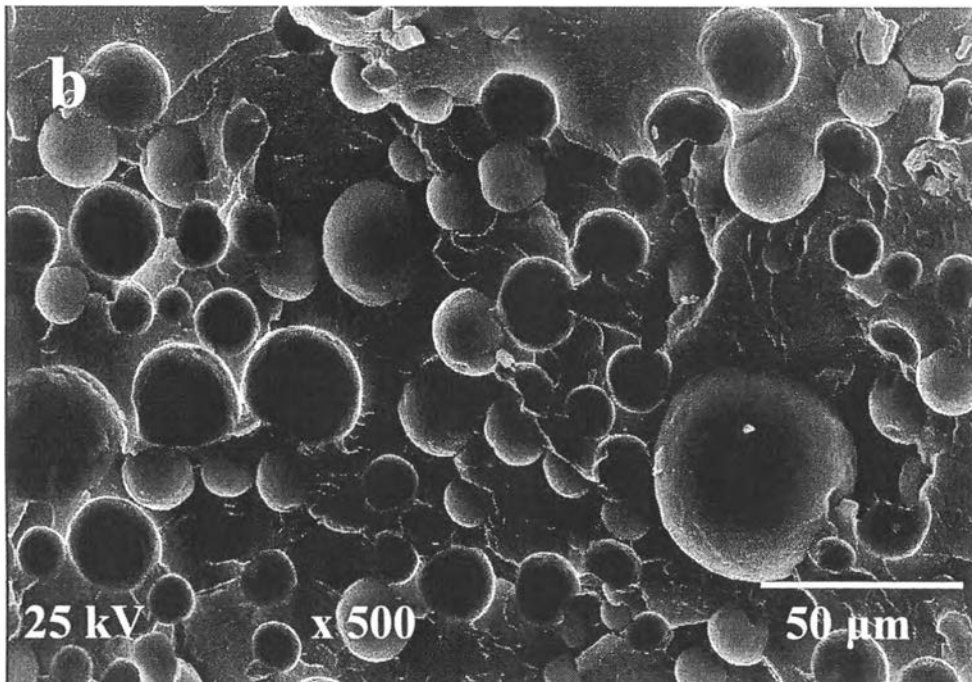
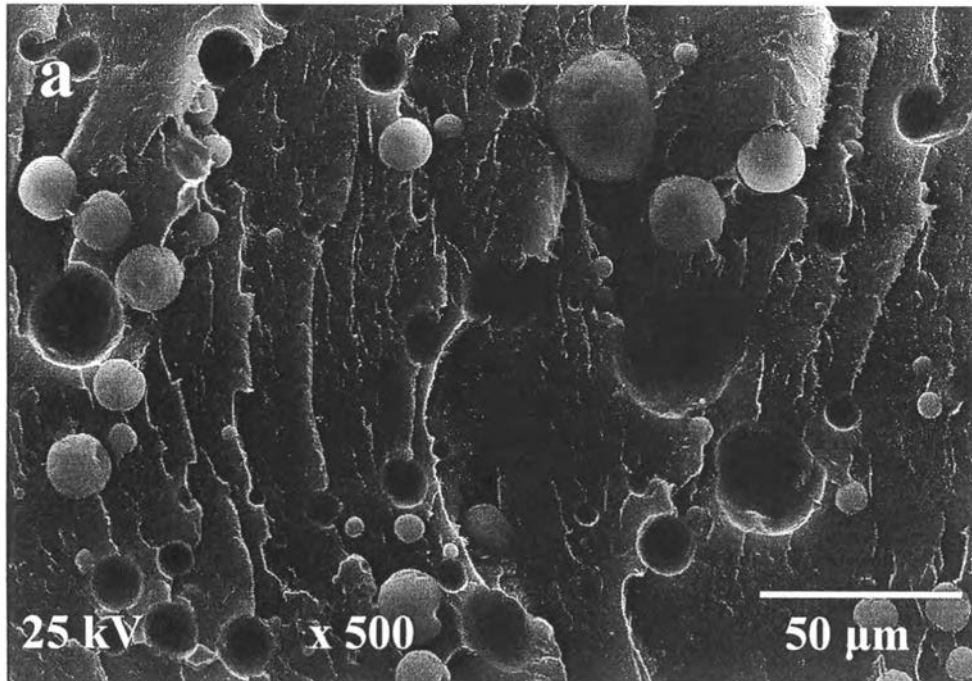
Table 5. Kinetic parameters of PA6/LDPE with 0.5, 1.5, and 5.0 phr Surlyn®.

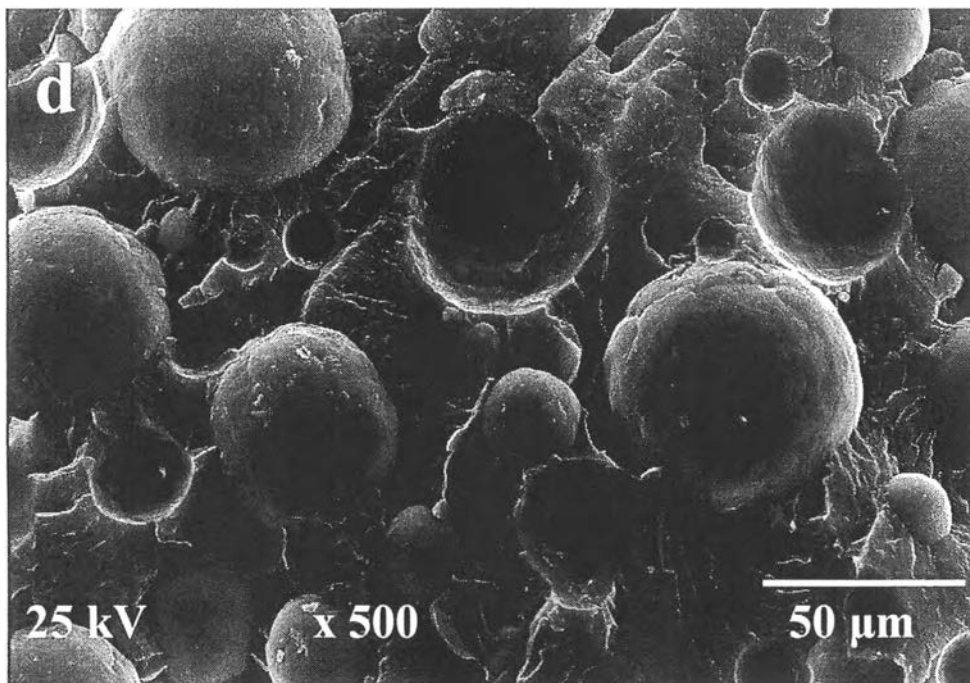
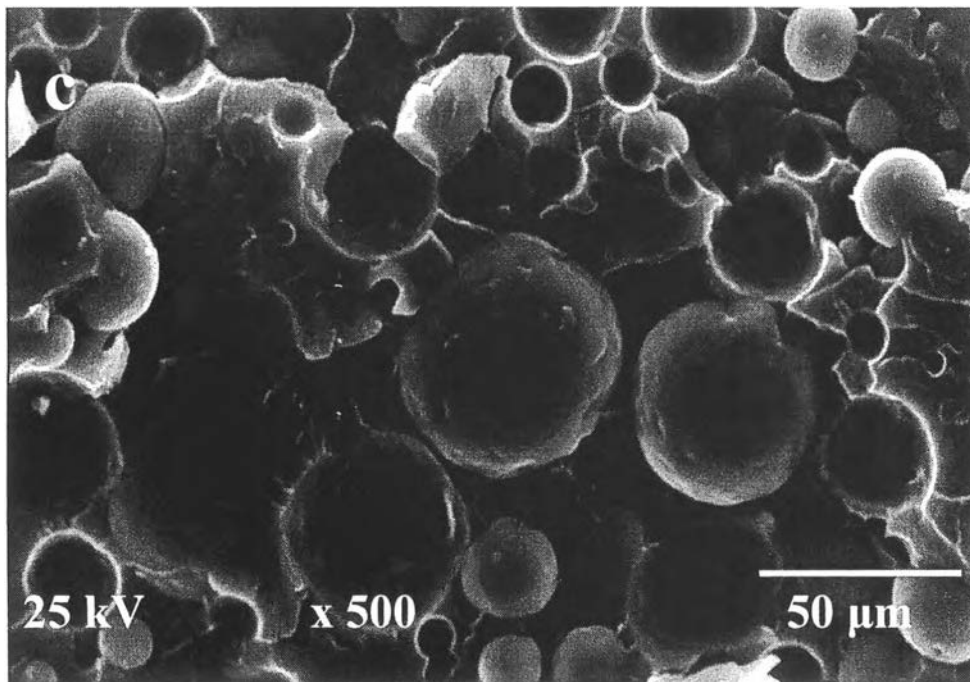
Surlyn® content	PA6/LDPE blend ratio	Degradation temperature at 0.1 fractional conversion (°C)	E _a (kJ/mol)	ln A (ln min ⁻¹)
0.5 phr	20/80	271.5	58.5	8.6
	40/60	295.6	55.38	11.3
	50/50	327.2	80.23	12.8
	60/40	321.4	78.1	11.9
	80/20	335.3	77.56	26.5
1.5 phr	20/80	277.4	59.6	9.2
	40/60	321.0	63.0	12.4
	50/50	313.8	68.36	17.2
	60/40	331.2	95.39	20.6
	80/20	345.7	115.9	21.5
5.0 phr	20/80	292.6	64.7	9.7
	40/60	328.0	80.1	13.8
	50/50	324.1	81.4	21.3
	60/40	338.9	141.9	25.7
	80/20	351.5	176.9	29.9

LIST OF FIGURE

- Figure 1 Scanning electron micrographs of fractured surfaces of noncompatibilized PA6/LDPE blends: (a) 20/80,(b) 40/60, (c) 50/50, (d) 60/40, and (e) 80/20
- Figure 2 Scanning electron micrographs of fractured surfaces of compatibilized PA6/LDPE blends at ratio 20/80: (a) with 0.5 phr Surlyn[®] and (b) with 5 phr Surlyn[®]
- Figure 3 Scanning electron micrographs of fractured+etched surfaces of 80/20 PA6/LDPE blends after immersion in decalin: (a) without Surlyn[®] (b) with 0.5 phr Surlyn[®], (c) with 1.5 phr Surlyn[®], and (d) with 5 phr Surlyn[®]
- Figure 4 Scanning electron micrographs of fractured surfaces of compatibilized PA6/LDPE blends: (a) 40/60 and (b) 50/50
- Figure 5 Scanning electron micrographs of fractured surfaces of PA6/Surlyn[®] blends
- Figure 6 Scanning electron micrographs of fractured+etched surfaces of PA6/Surlyn[®] blends (a) 20/80, (b) 40/60, (c) 50/50, (d) 60/40, and (e) 80/20
- Figure 7 Scanning electron micrographs of fractured surfaces of Surlyn[®]/LDPE blends: (a) 20/80, (b) 40/60, (c) 50/50, (d) 60/40, and (e) 80/20
- Figure 8 WAXS patterns of PA6/LDPE blends: (a) 20/80, (b) 40/60, (c) 50/50, (d) 60/40, and (e) 80/20
- Figure 9 WAXS patterns of PA6/Surlyn[®] blends: (a) 20/80, (b) 40/60, (c) 50/50, (d) 60/40, and (e) 80/20
- Figure 10 WAXS patterns of Surlyn[®]/LDPE blends: (a) 20/80, (b) 40/60, (c) 50/50, (d) 60/40, and (e) 80/20
- Figure 11 DSC thermograms of PA6/Surlyn[®] blends: (a) 20/80, (b) 40/60, (c) 50/50, (d) 60/40, and (e) 80/20
- Figure 12 DSC thermograms of Surlyn[®]/LDPE blends: (a) 20/80, (b) 40/60, (c) 50/50, (d) 60/40, and (e) 80/20

- Figure 13 DSC melting thermograms of PA6/LDPE blends: (a) 20/80, (b) 40/60, (c) 50/50, (d) 60/40, and (e) 80/20
- Figure 14 DSC crystallization thermograms of PA6/ Surlyn[®] blends: (a) 20/80, (b) 40/60, (c) 50/50, (d) 60/40, and (e) 80/20
- Figure 15 TGA thermograms of pure polymer: (a) LDPE, (b) PA6, and (c) Surlyn[®]
- Figure 16 Degradation temperature (0.1 fractional conversion) of blends (a) noncompatibilized PA6/LDPE, (b) PA6/LDPE with 0.5 phr Surlyn[®], (c) PA6/LDPE with 1.5 phr Surlyn[®], and (d) PA6/LDPE with 5.0 phr Surlyn[®] compared with values determined from (e) the rule of mixing
- Figure 17 Degradation temperature (0.1 fractional conversion): (a) PA6/Surlyn[®] blends compared with values determined from (b) the rule of mixing
- Figure 18 Degradation temperature (0.1 fractional conversion): (a) Surlyn[®]/LDPE blends compared with values determined from (b) the rule of mixing





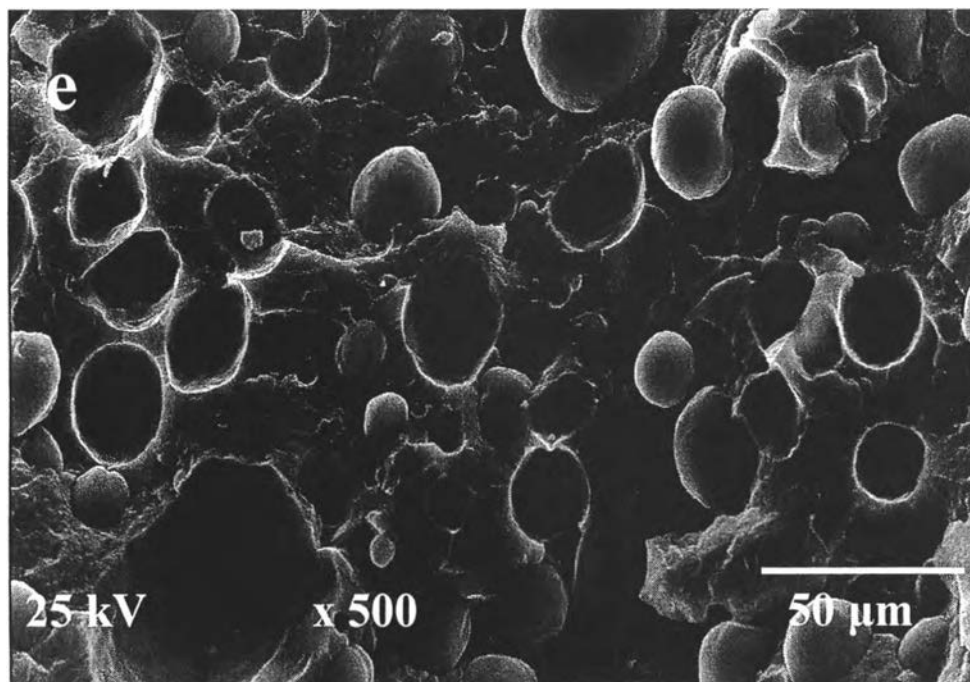


Figure 1. Scanning electron micrographs of fractured surfaces of noncompatibilized PA6/LDPE blends: (a) 20/80, (b) 40/60, (c) 50/50, (d) 60/40, and (e) 80/20.

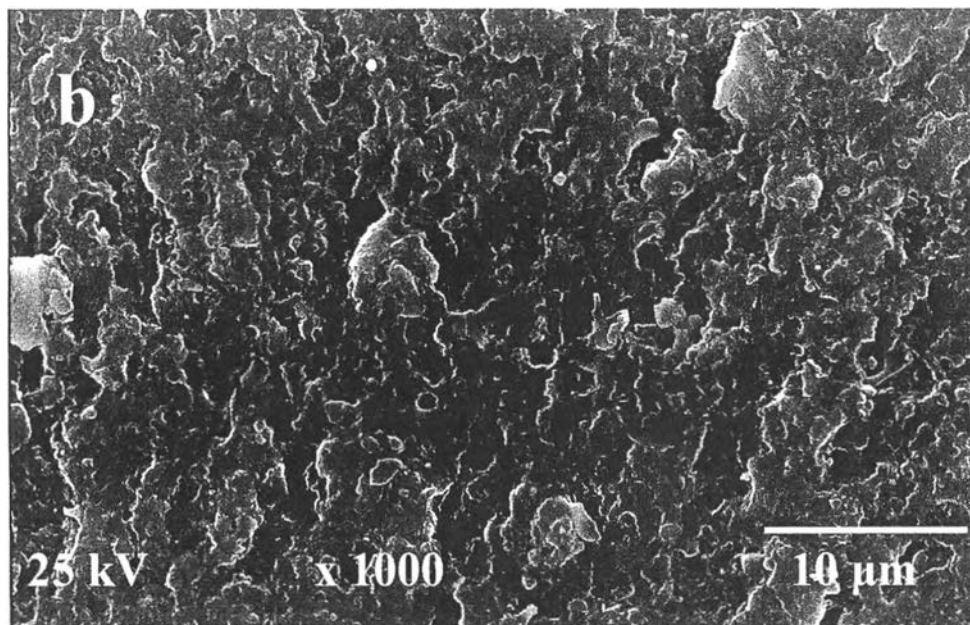
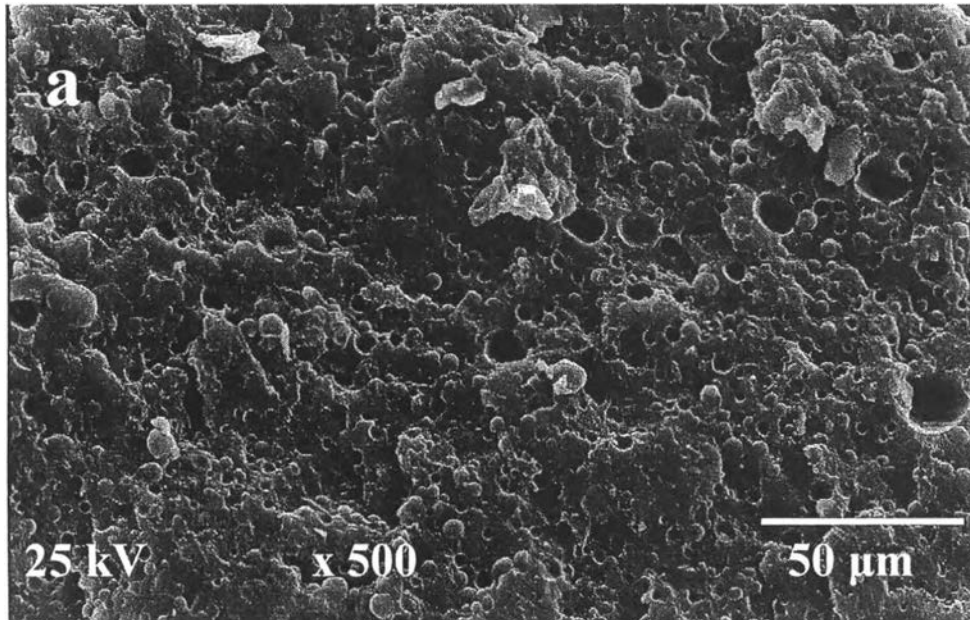
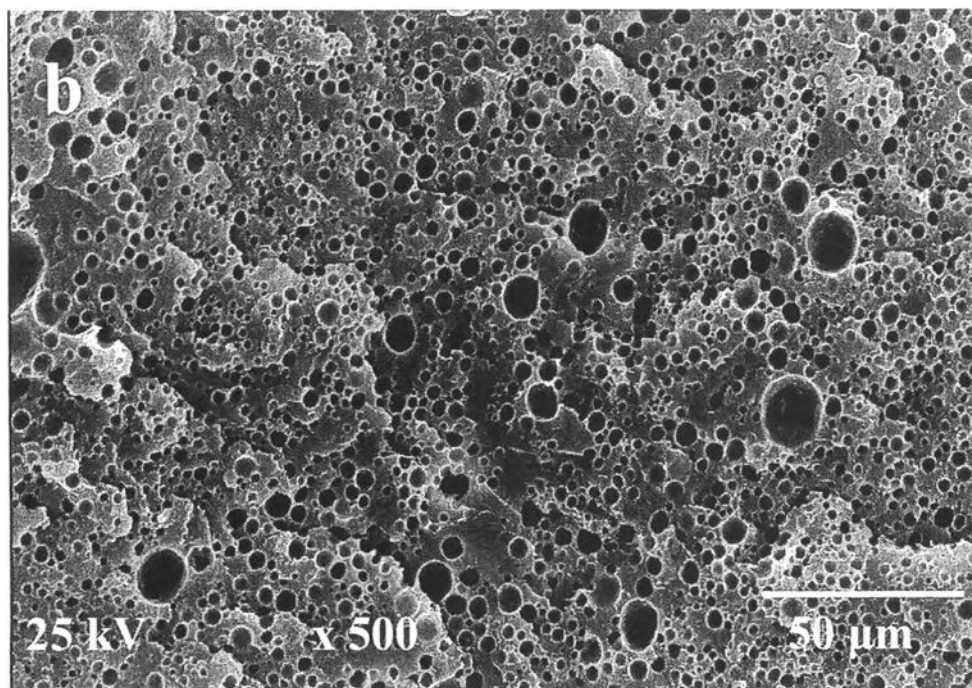
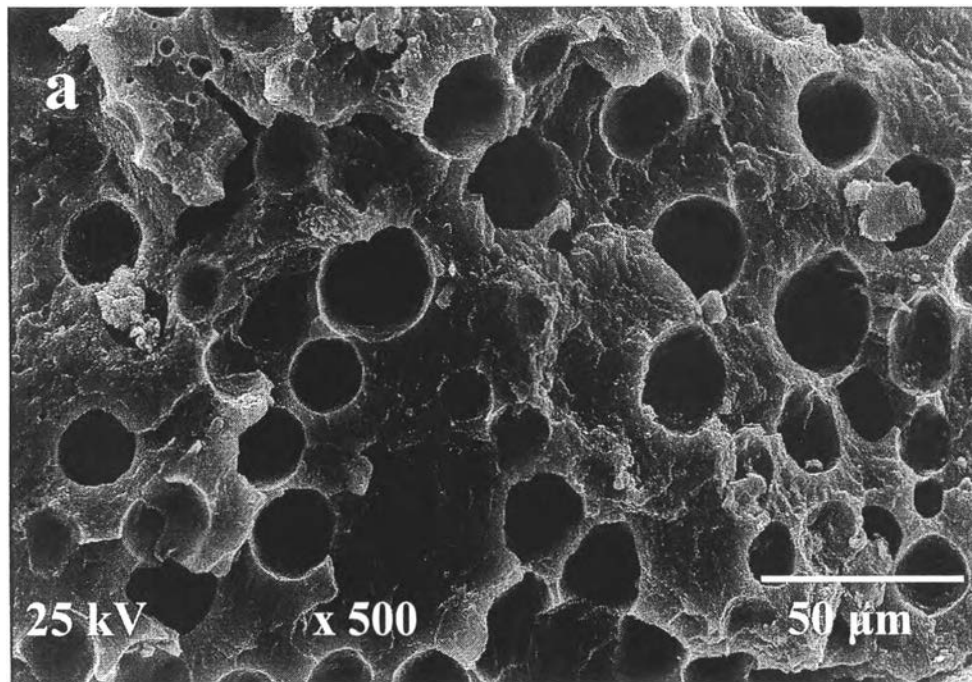


Figure 2. Scanning electron micrographs of fractured surfaces of compatibilized PA6/LDPE blends at ratio 20/80: (a) with 0.5 phr Surlyn[®] and (b) with 5 phr Surlyn[®].



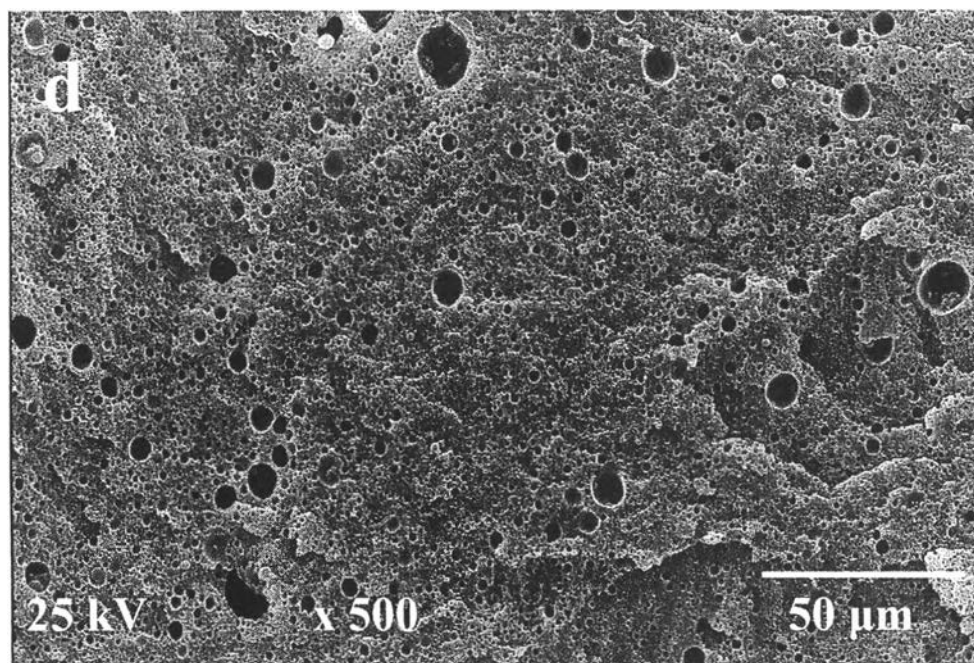
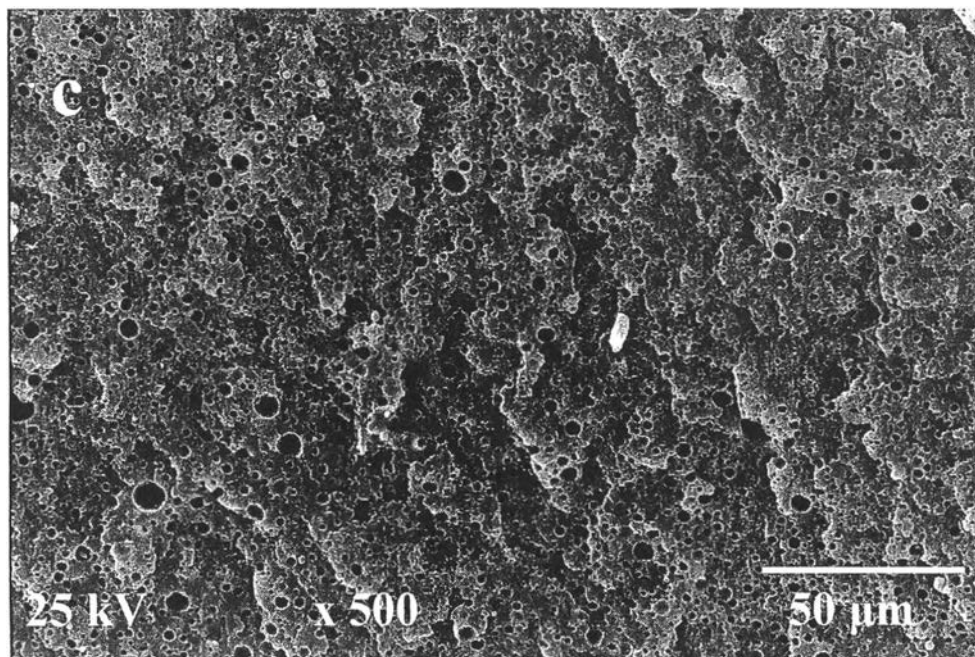


Figure 3. Scanning electron micrographs of fractured+etched surfaces of 80/20 PA6/LDPE blends after immersion in decalin: (a) without Surlyn[®] (b) with 0.5 phr Surlyn[®], (c) with 1.5 phr Surlyn[®], and (d) with 5 phr Surlyn[®].

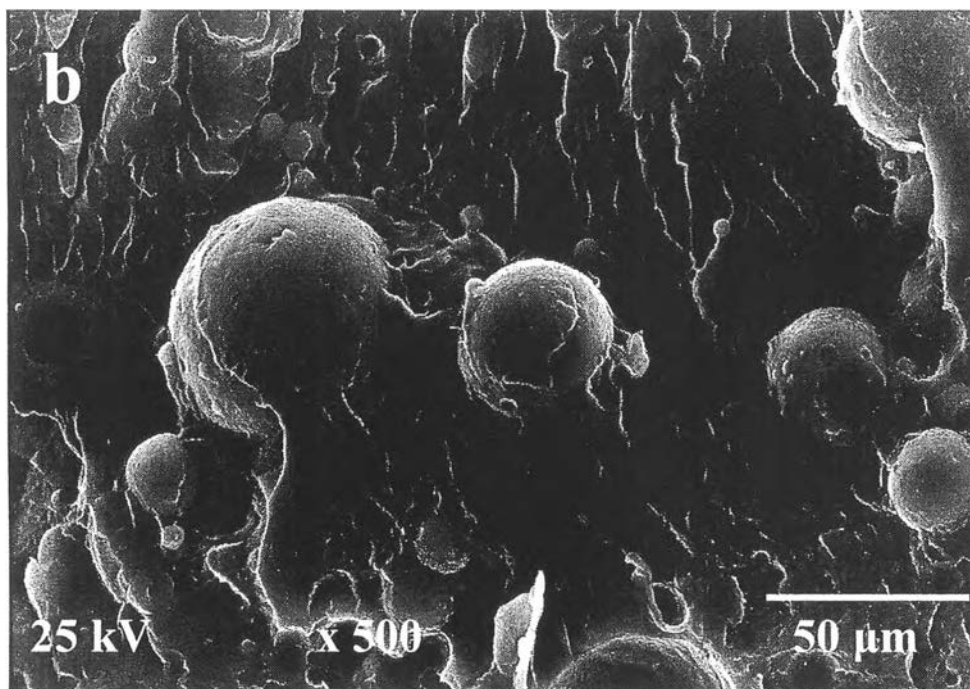
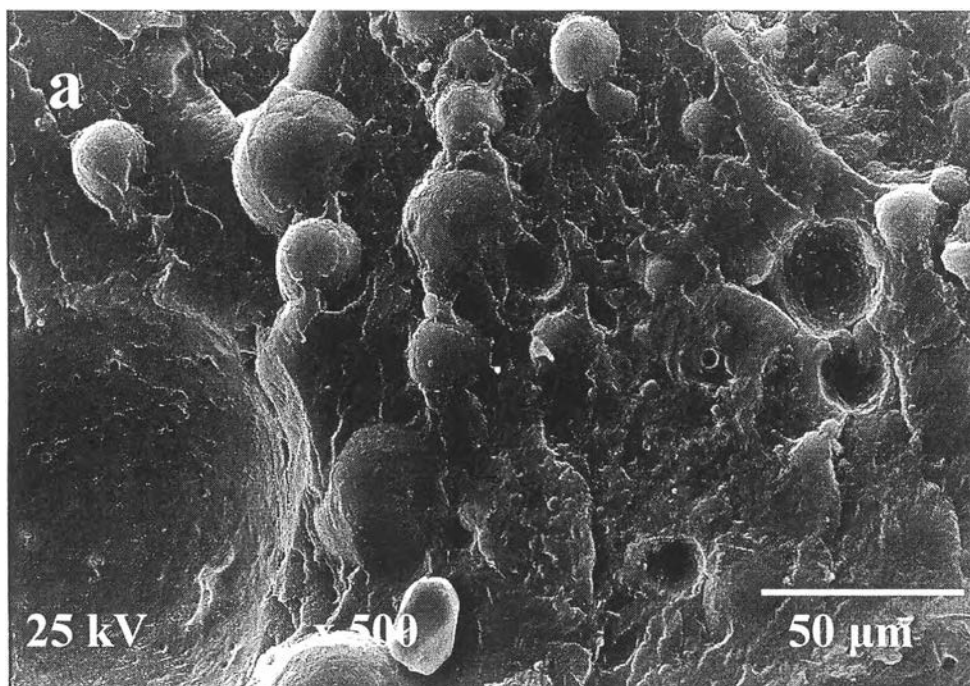


Figure 4. Scanning electron micrographs of fractured surfaces of compatibilized PA6/LDPE blends: (a) 40/60 and (b) 50/50.

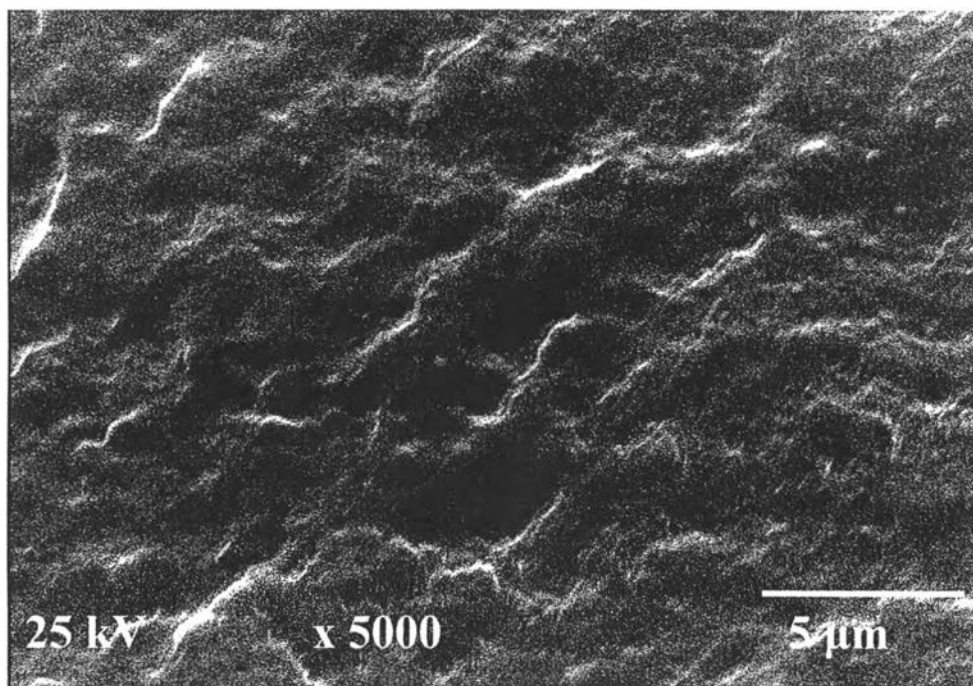
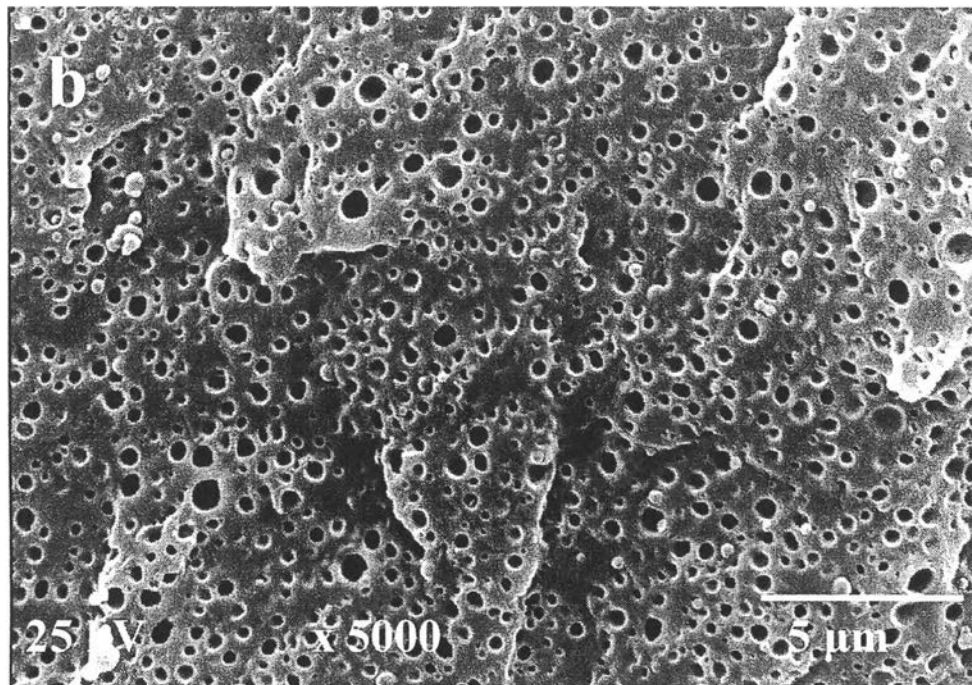
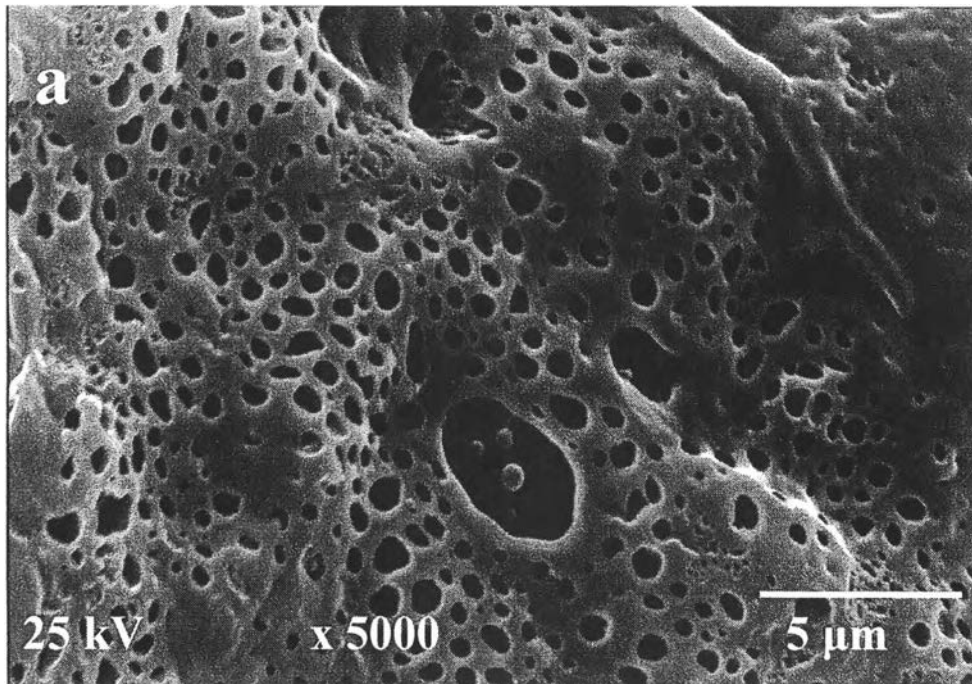
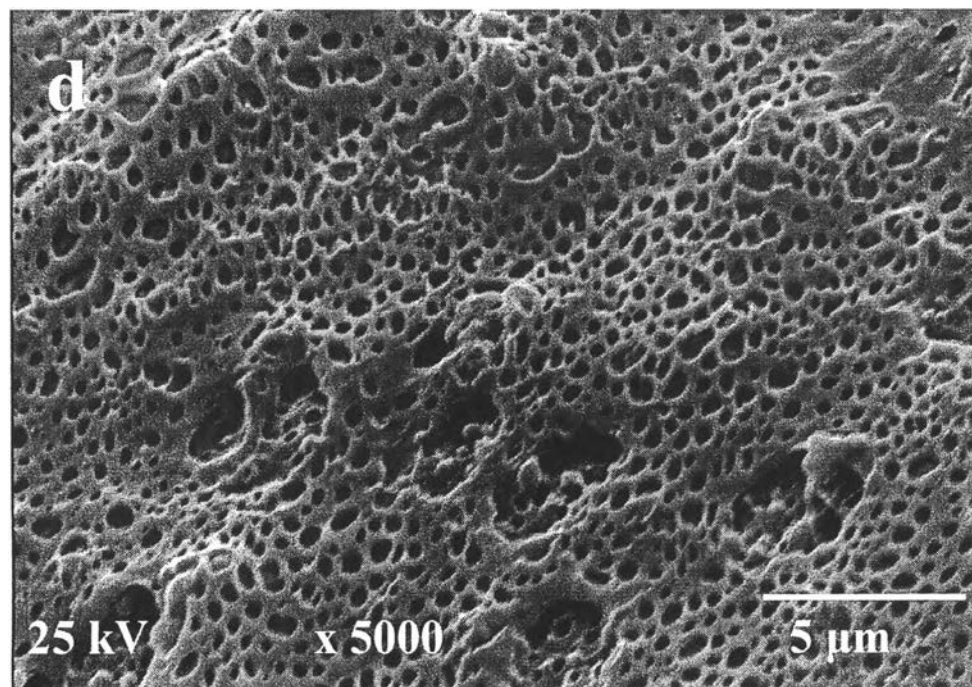
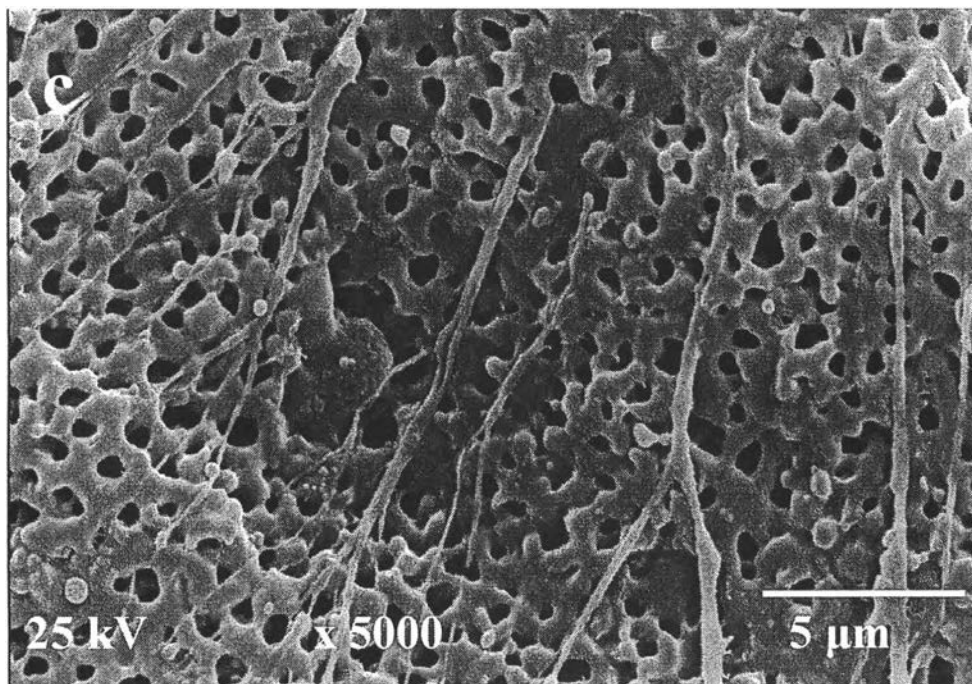


Figure 5. Scanning electron micrograph of fractured surface of PA6/Surlyn[®] 40/60 blend ratio.





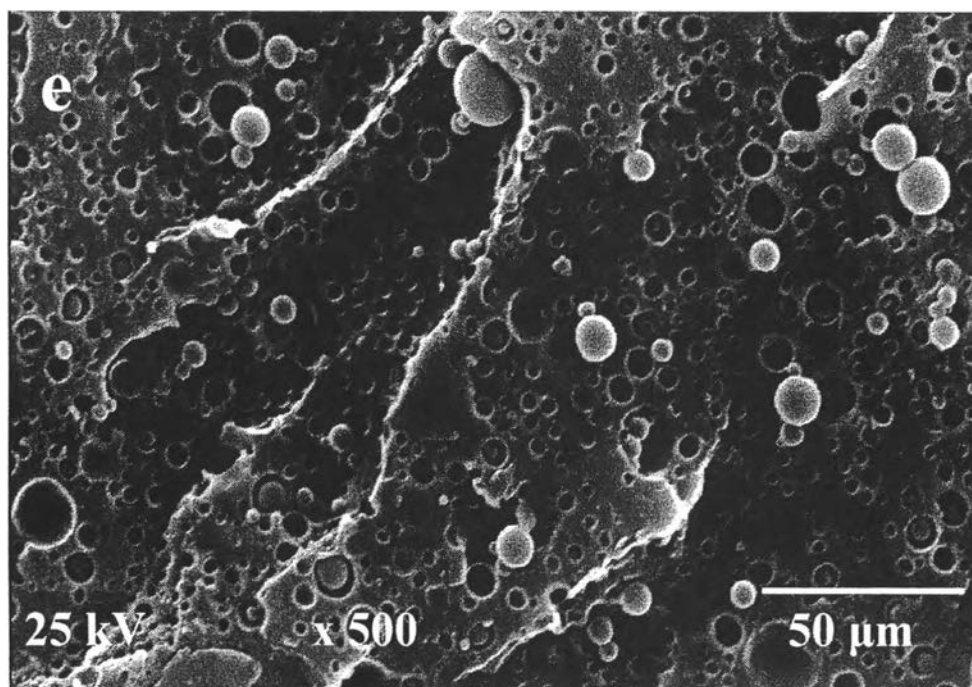
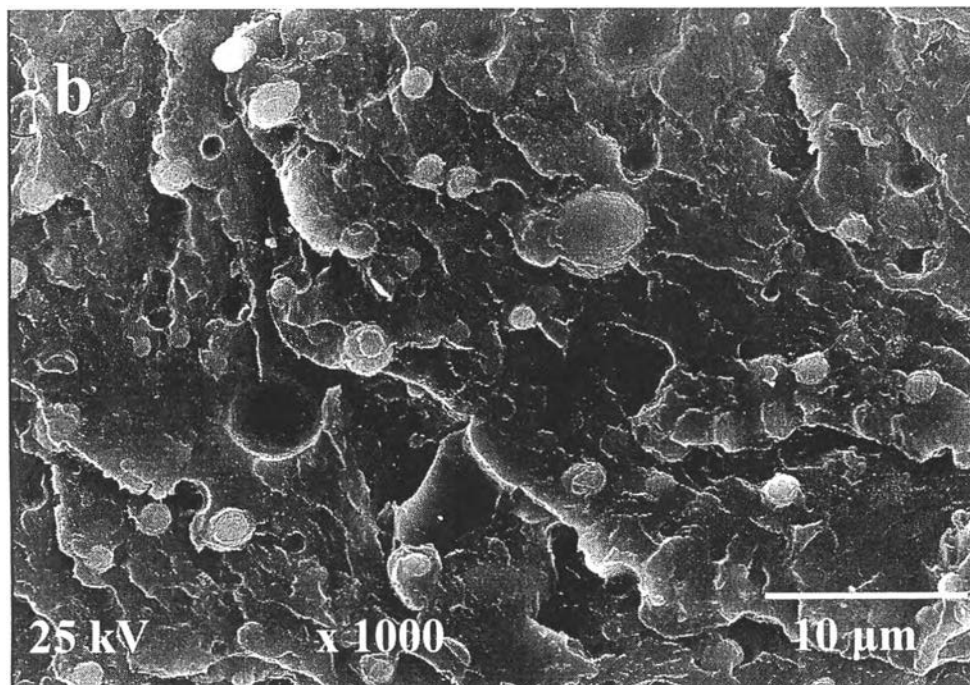
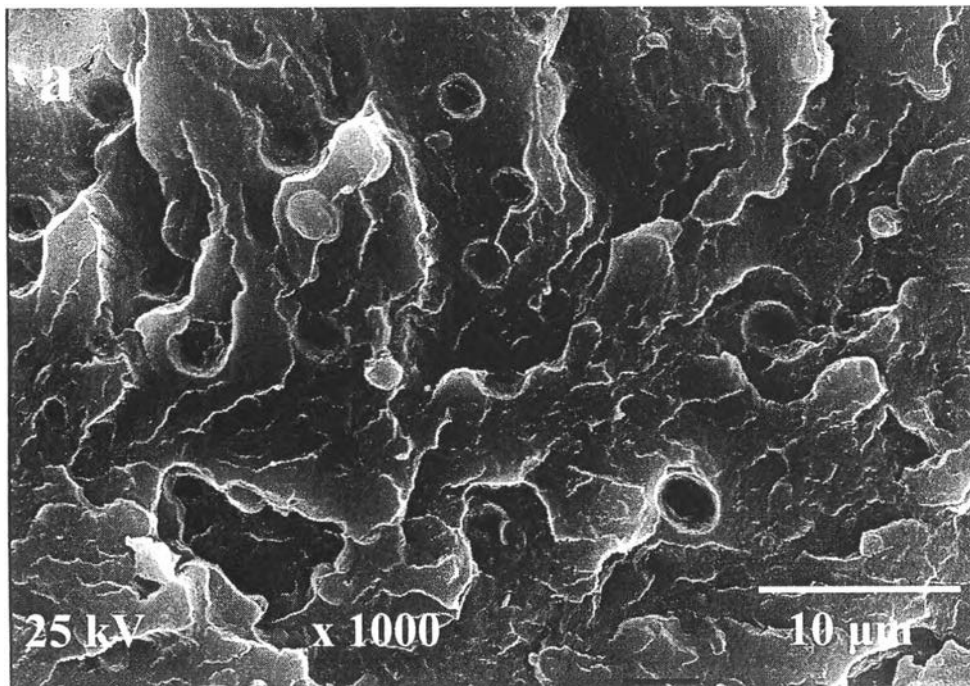
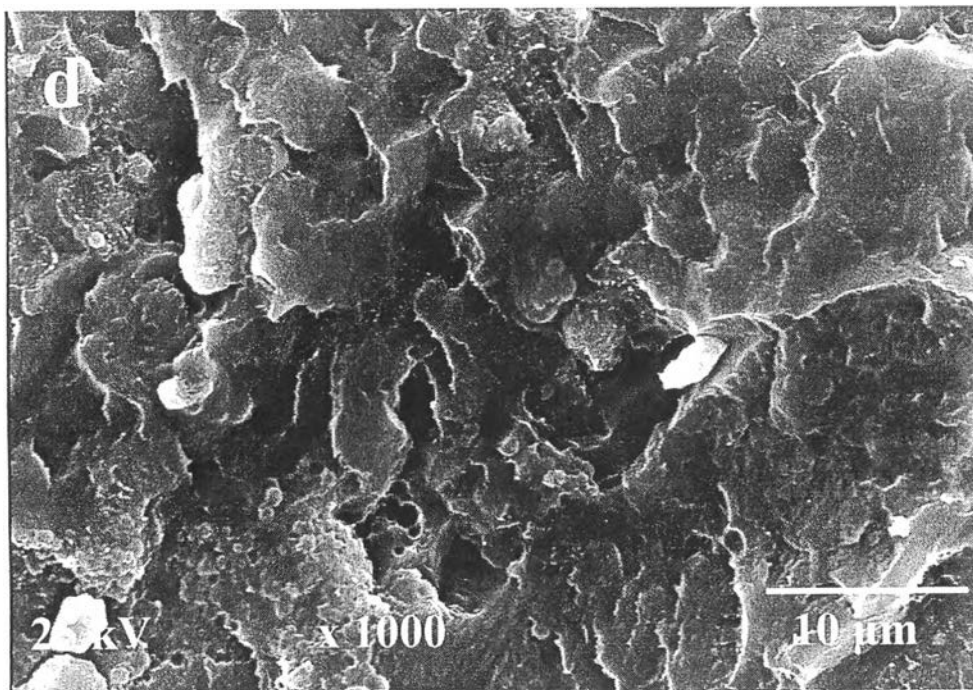
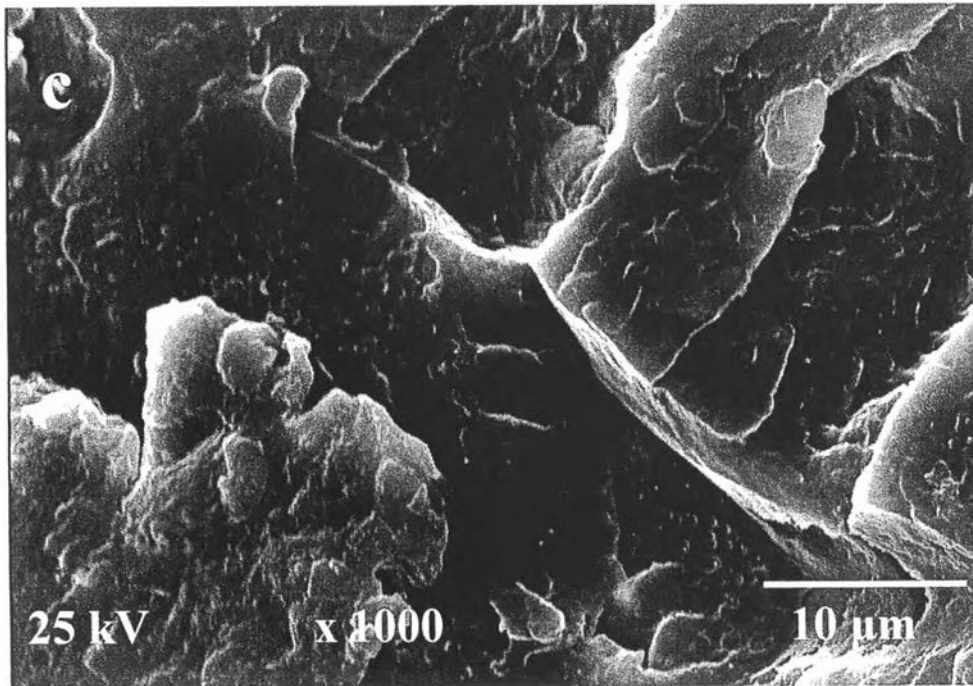


Figure 6. Scanning electron micrographs of fractured+etched surfaces of PA6/Surlyn[®] blends (a) 20/80, (b) 40/60, (c) 50/50, (d) 60/40, and (e) 80/20.





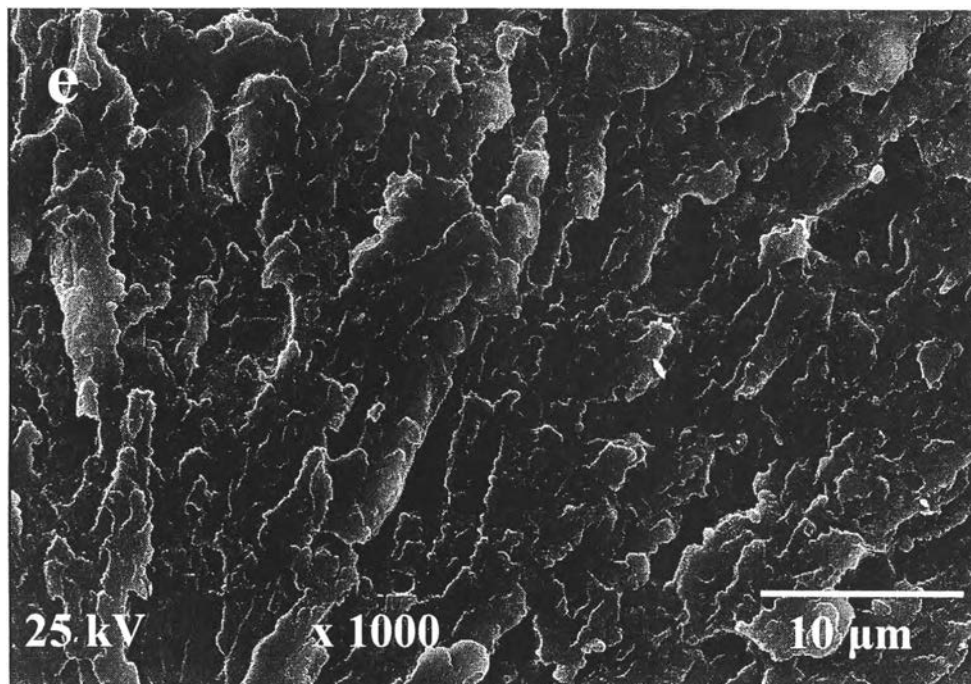


Figure 7. Scanning electron micrographs of fractured surfaces of Surlyn[®]/LDPE blends: (a) 20/80, (b) 40/60, (c) 50/50, (d) 60/40, and (e) 80/20.

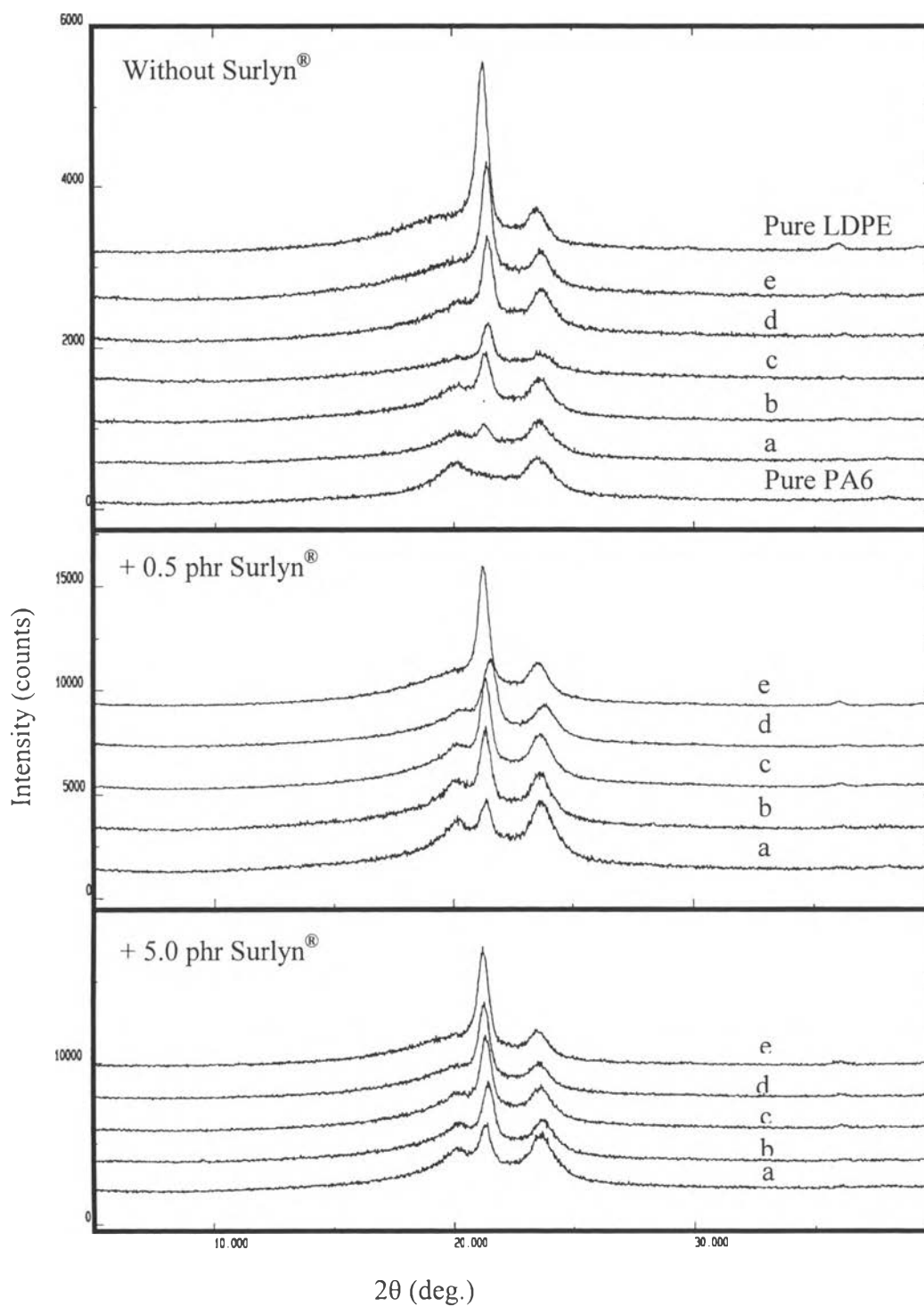


Figure 8. WAXS patterns of PA6/LDPE blends: (a) 20/80, (b) 40/60, (c) 50/50, (d) 60/40, and (e) 80/20.

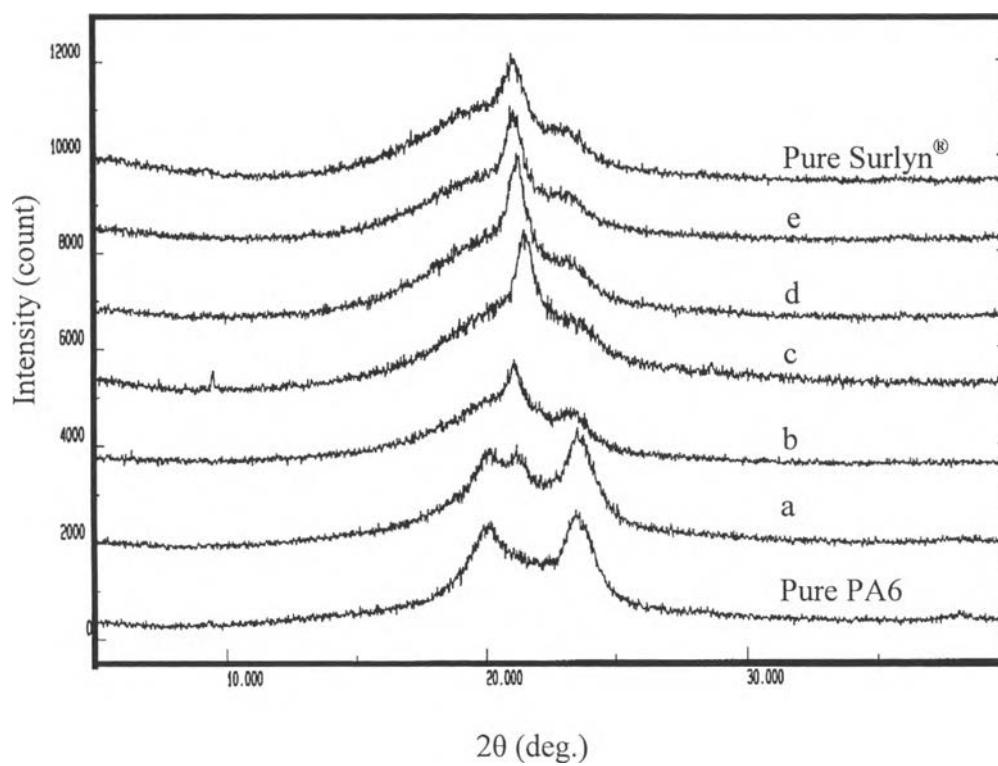


Figure 9. WAXS patterns of PA6/Surlyn[®] blends: (a) 20/80, (b) 40/60, (c) 50/50, (d) 60/40, and (e) 80/20.

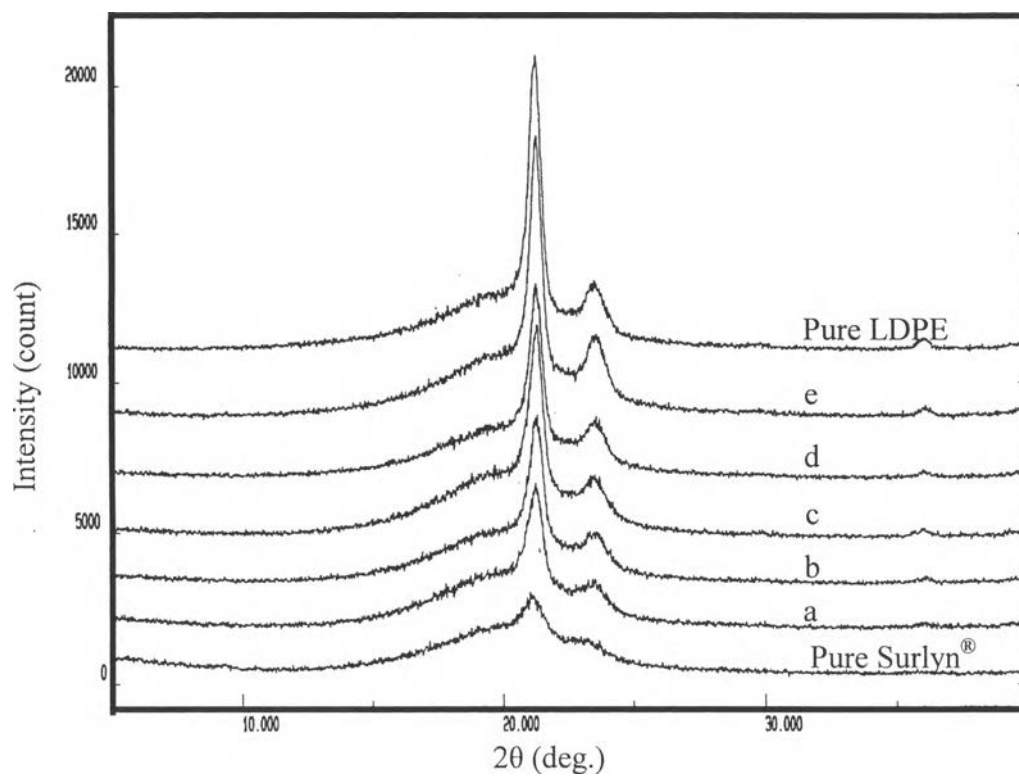


Figure 10. WAXS patterns of Surlyn[®]/LDPE blends: (a) 20/80, (b) 40/60, (c) 50/50, (d) 60/40, and (e) 80/20.

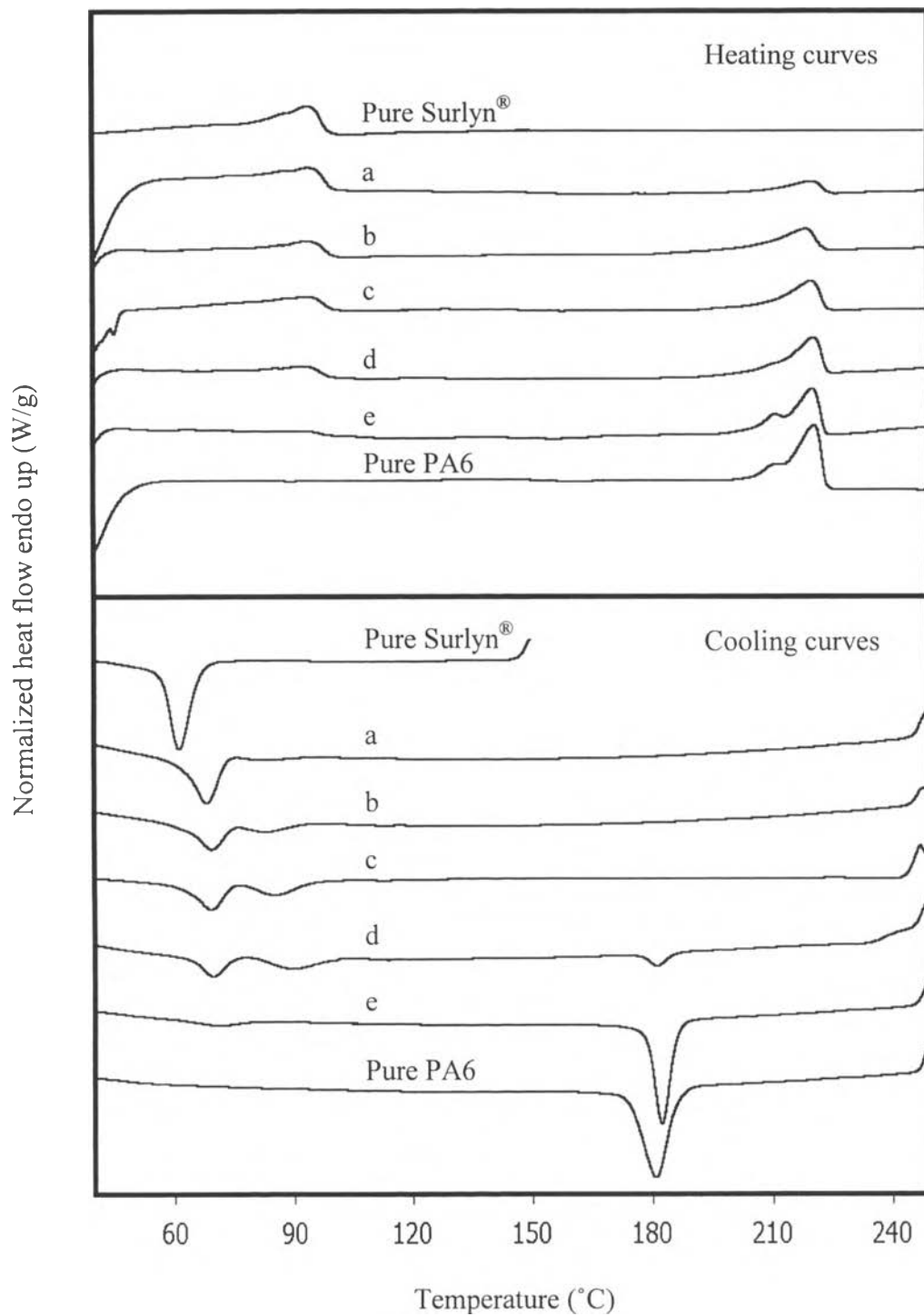


Figure 11. DSC thermograms of PA6/Surlyn[®] blends: (a) 20/80, (b) 40/60, (c) 50/50, (d) 60/40, and (e) 80/20.

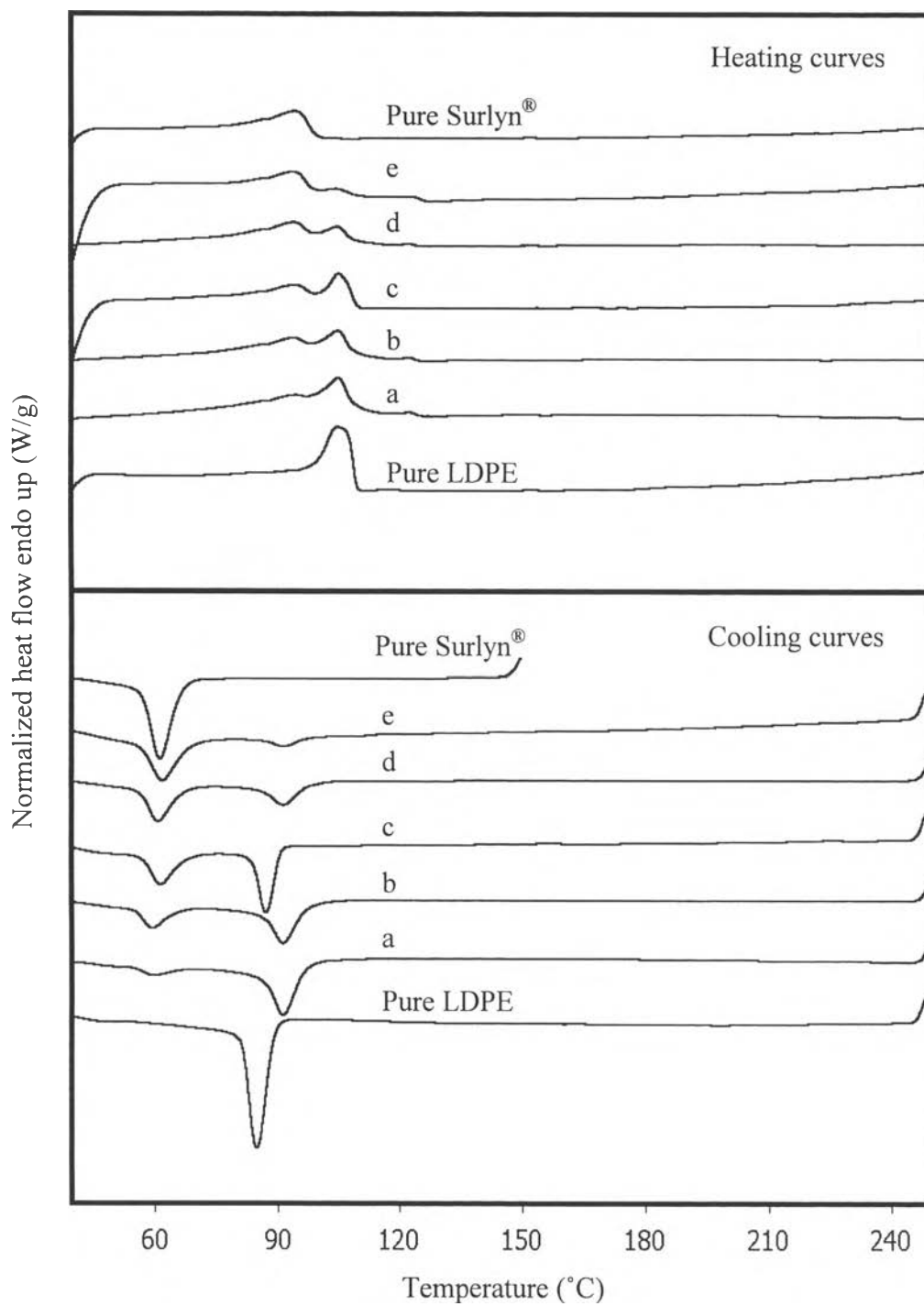


Figure 12. DSC thermograms of Surlyn[®]/LDPE blends: (a) 20/80, (b) 40/60, (c) 50/50, (d) 60/40, and (e) 80/20.

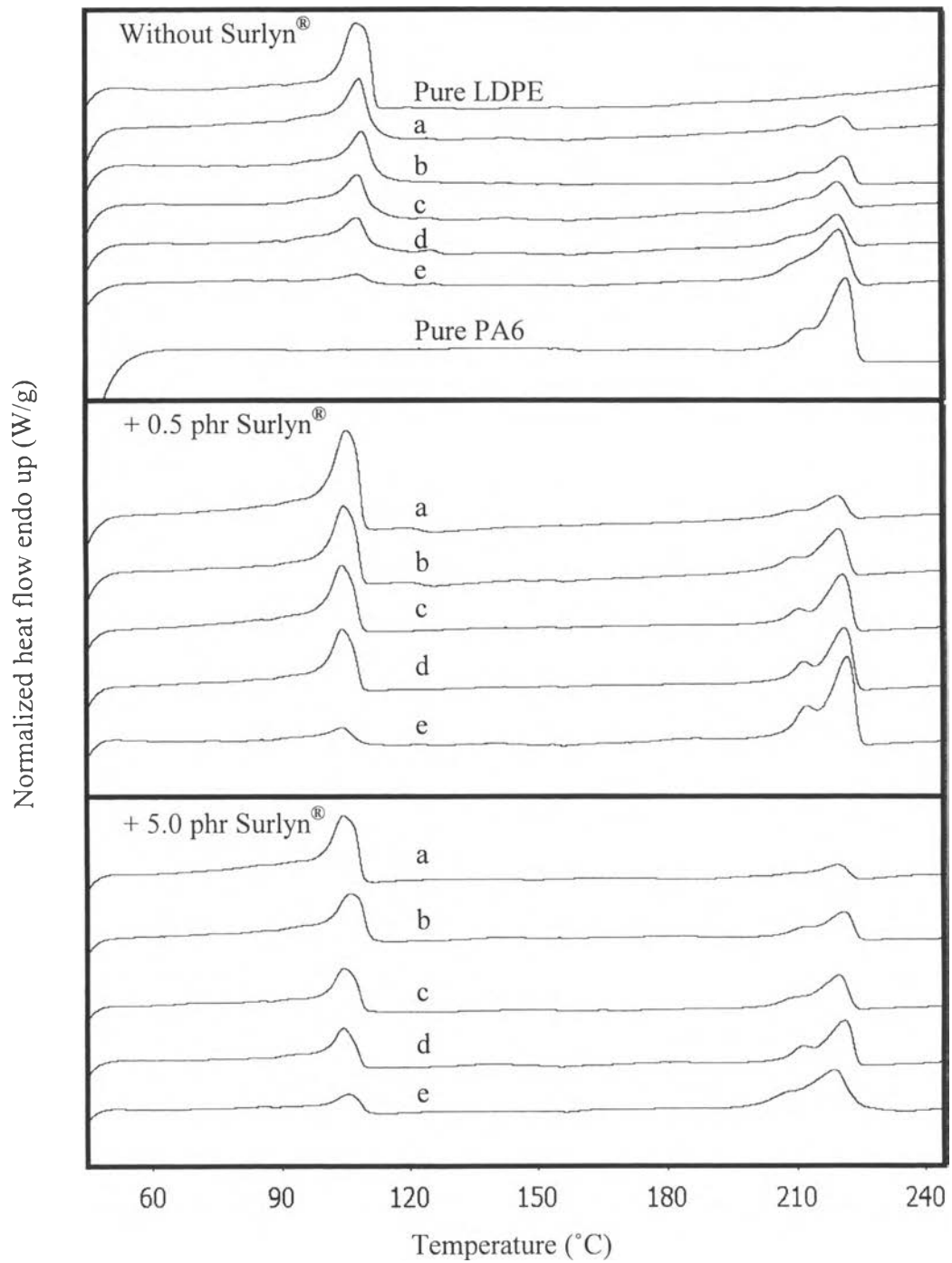


Figure 13. DSC melting thermograms of PA6/LDPE blends: (a) 20/80, (b) 40/60, (c) 50/50, (d) 60/40, and (e) 80/20.

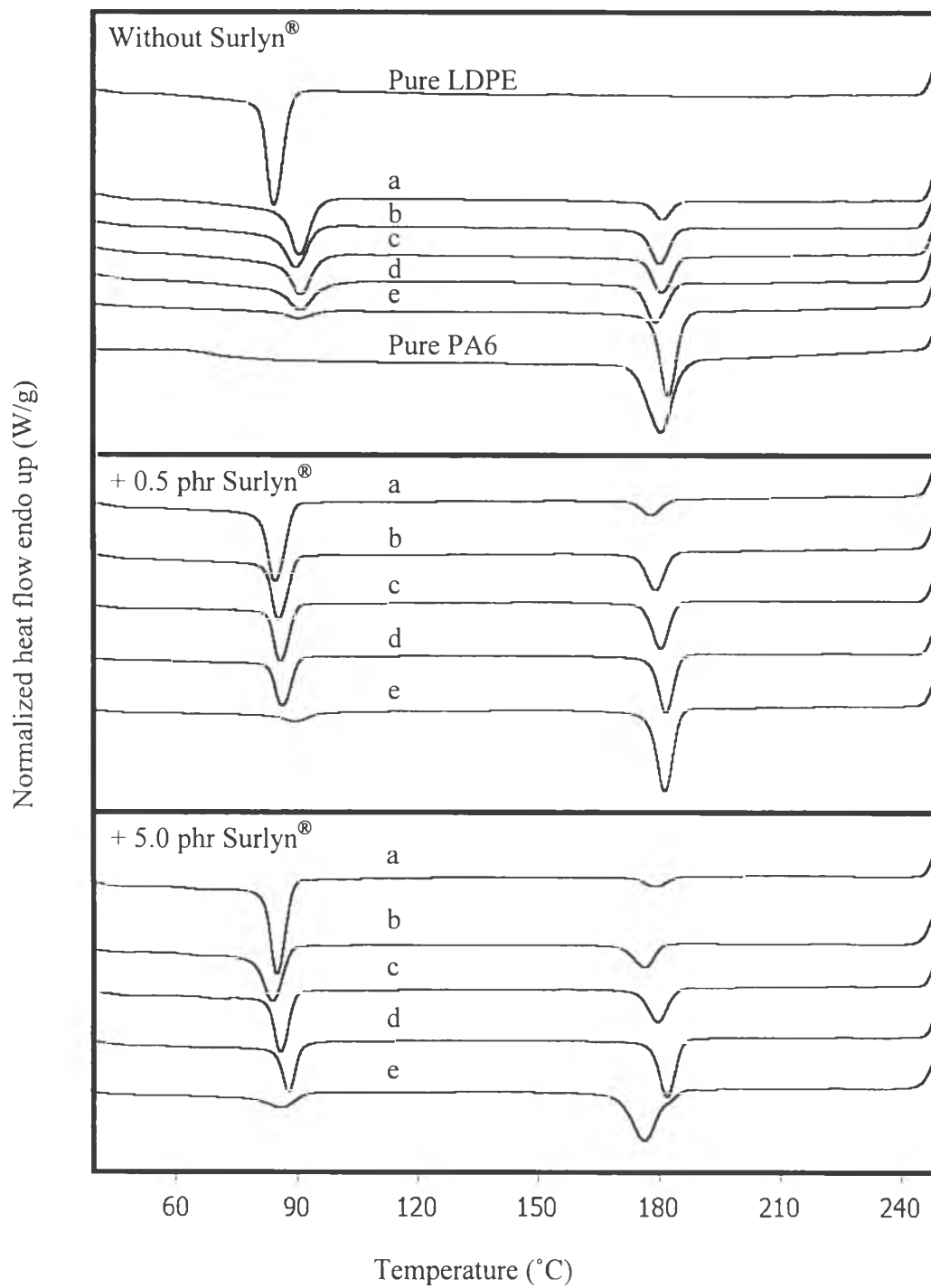


Figure 14. DSC crystallization thermograms of PA6/ionomer blends: (a) 20/80, (b) 40/60, (c) 50/50, (d) 60/40, and (e) 80/20.

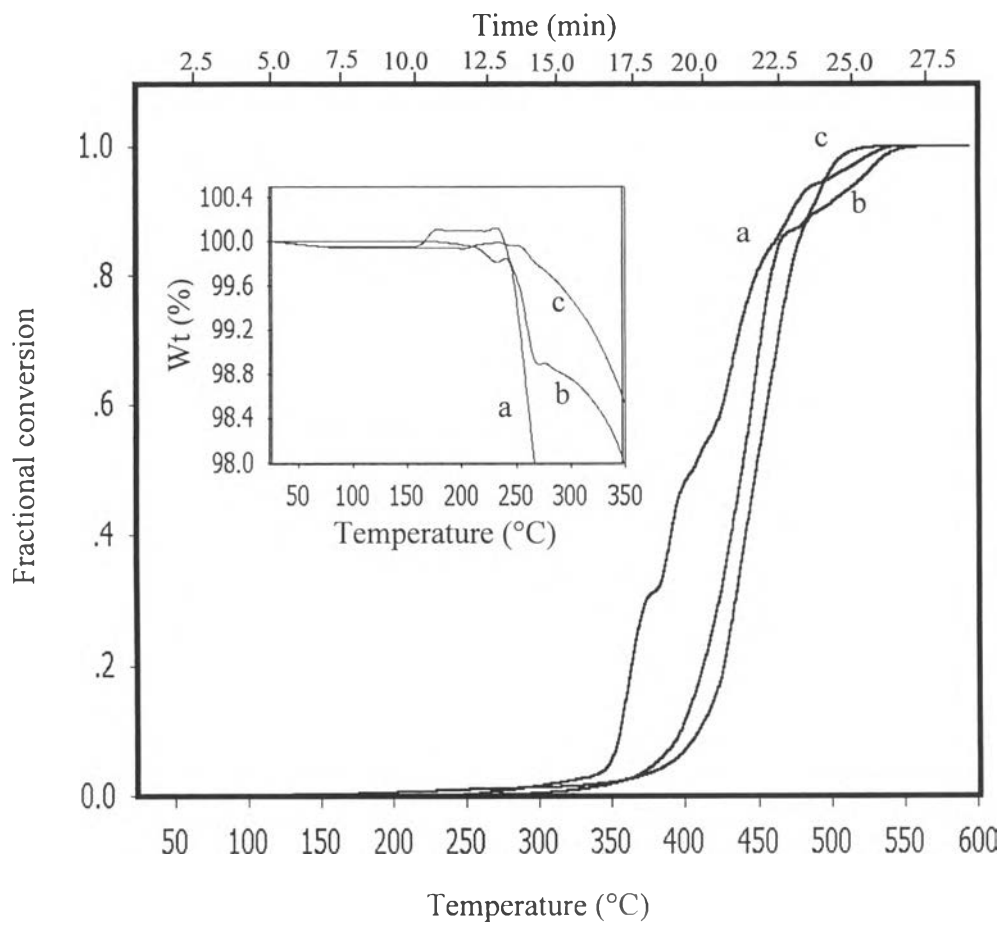


Figure 15. TGA thermograms of pure polymer: (a) LDPE, (b) PA6, and (c) Surlyn®.

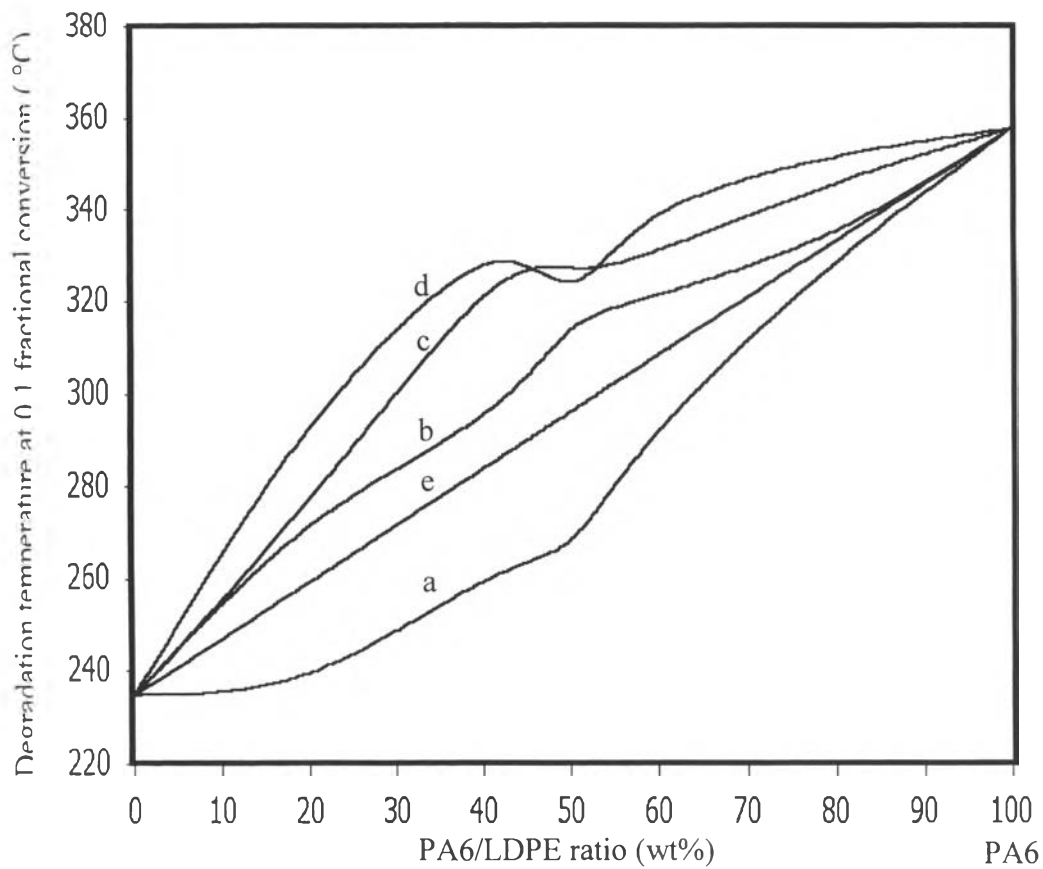


Figure 16. Degradation temperature (0.1 fractional conversion) of blends: (a) noncompatibilized PA6/LDPE, (b) PA6/LDPE with 0.5 phr Surlyn[®], (c) PA6/LDPE with 1.5 phr Surlyn[®], and (d) PA6/LDPE with 5.0 phr Surlyn[®] compared with values determined from (e) the rule of mixing.

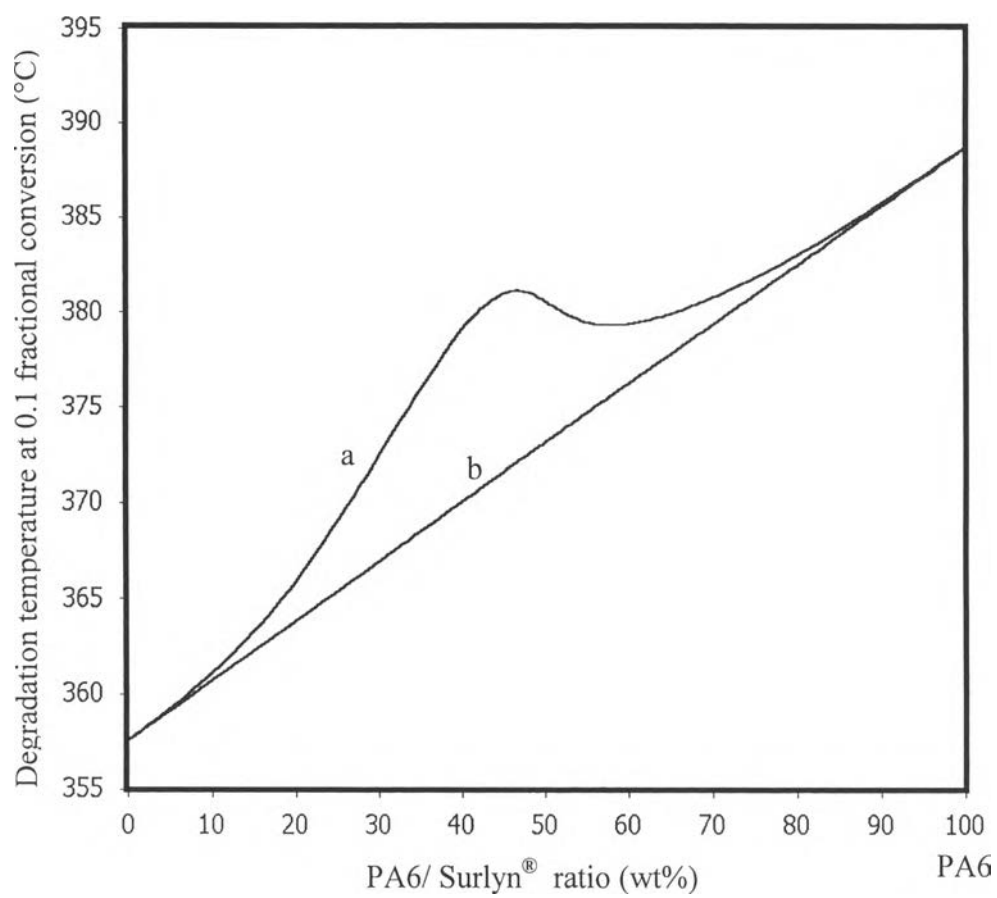


Figure 17. Degradation temperature (0.1 fractional conversion) of blends: (a) PA6/Surlyn® compared with values determined from (b) the rule of mixing.

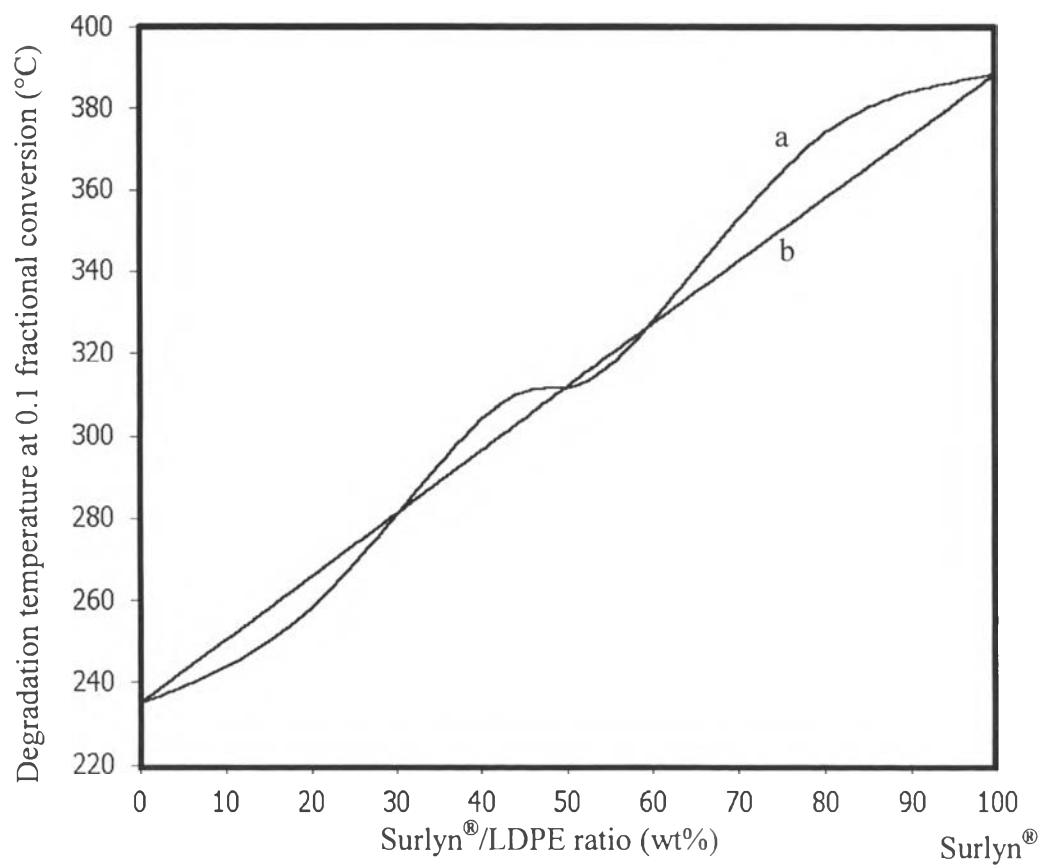


Figure 18. Degradation temperature (0.1 fractional conversion) of blends: (a) Surlyn[®]/LDPE compared with values determined from (b) the rule of mixing.